Rheology

Experimental data

- Steady shear flow
  - General effects
  - Material effects
  - Temp and press effects
- Unsteady shear flow
  - Small strain
  - Large strain
- Elongational flow

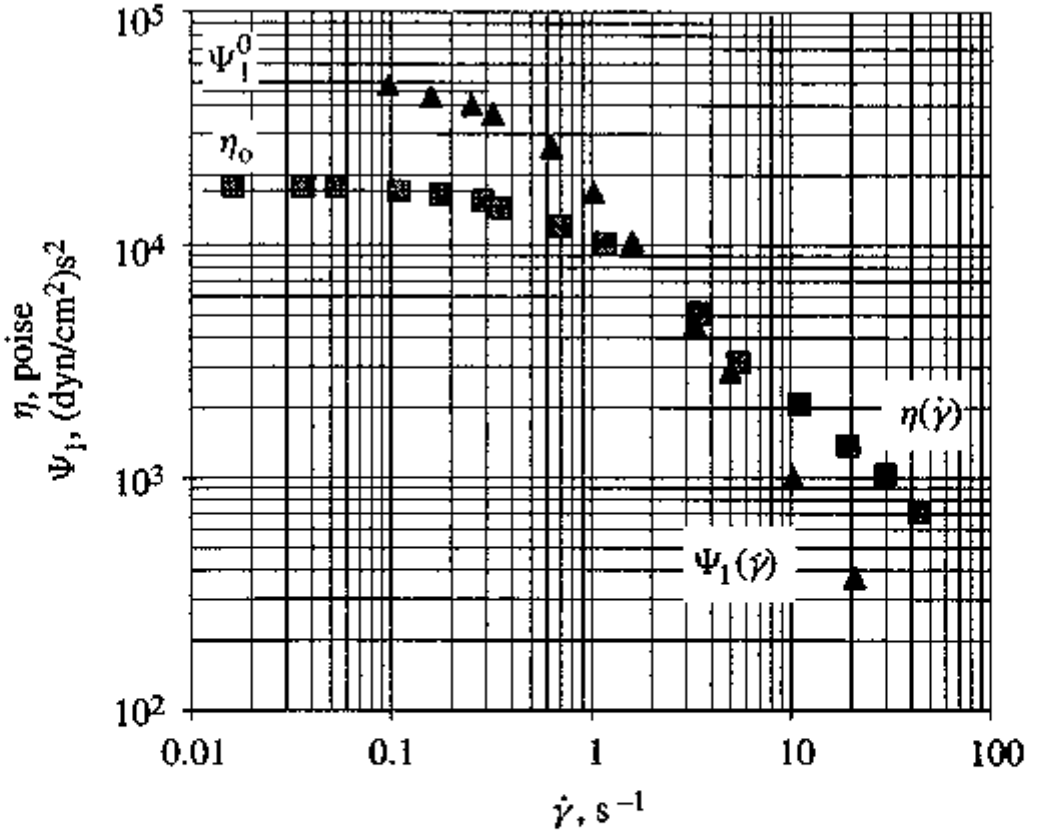

Figure 6.1 Steady shear viscosity η and first normal-stress coefficient Ψ_1 as a function of shear rate $\dot{\gamma}$ for a concentrated solution of a narrowly distributed polybutadiene; replotted from Menezes and Graessley [177]. $M_w = 350$ kg/mol; $M_w/M_n < 1.05$; concentration = 0.0676 g/cm^3 in Flexon 391, a hydrocarbon oil. *Source:* From "Nonlinear rheological behavior of polymer systems for several shear-flow histories," by E. V. Menezes and W. W. Graessley, *Journal of Polymer Science, Polymer Physics Edition*, Copyright © 1982 by John Wiley & Sons, Inc. Reprinted by permission of John Wiley & Sons, Inc.

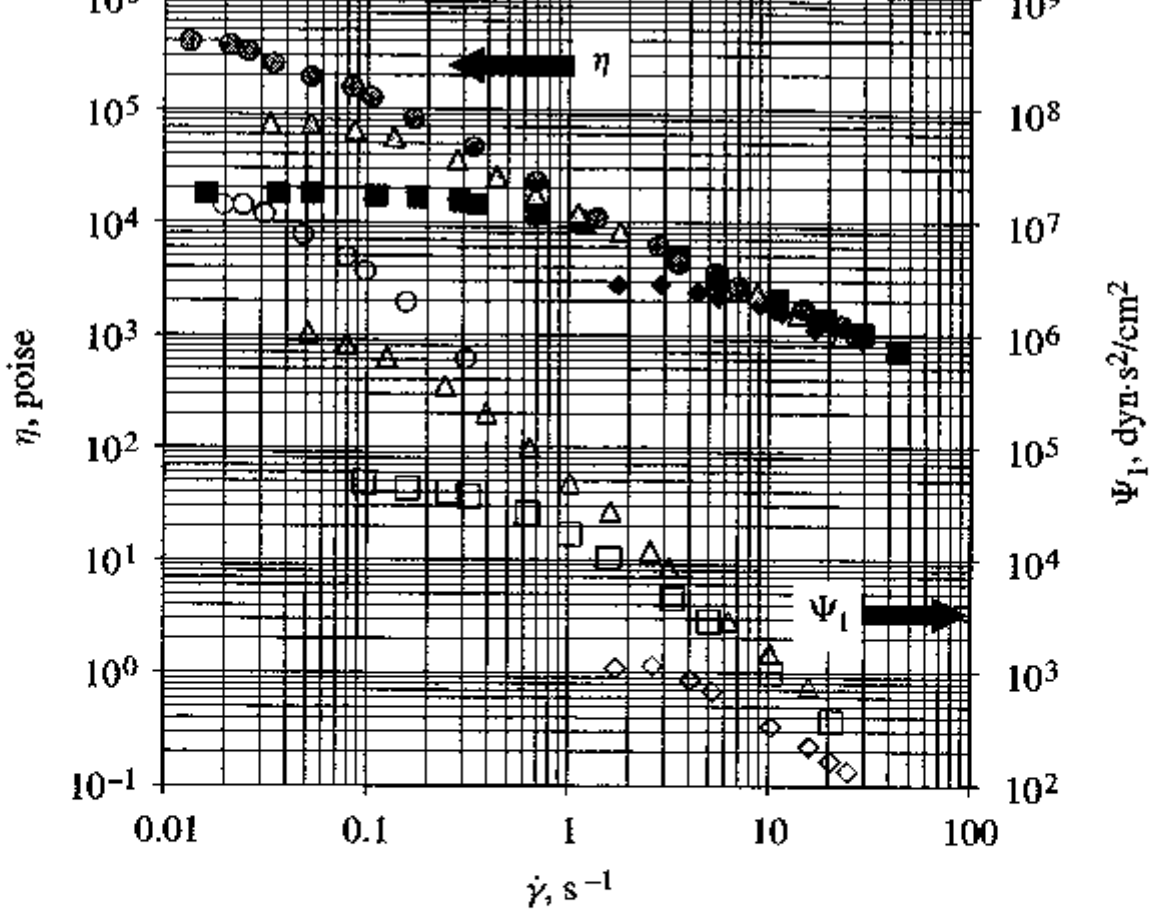

Figure 6.2 Steady shear viscosity η and first normal-stress coefficient Ψ_1 as a function of shear rate $\dot{\gamma}$ for concentrated solutions of four narrowly distributed polybutadienes; replotted from Menezes and Graessley [177]. Filled symbols are viscosity η; open symbols are first normal-stress coefficient Ψ_1. ◇, $M_w = 200$ kg/mol; □, $M_w = 350$ kg/mol; △, $M_w = 517$ kg/mol; ○, $M_w = 813$ kg/mol. For all materials $M_w/M_n < 1.05$; concentration = 0.0676 g/cm^3 in Flexon 391, a hydrocarbon oil. Note that the Ψ_1 data are displayed three decades lower than the η data. *Source:* From "Nonlinear rheological behavior of polymer systems for several shear-flow histories," by E. V. Menezes and W. W. Graessley, *Journal of Polymer Science, Polymer Physics Edition*, Copyright © 1982 by John Wiley & Sons, Inc. Reprinted by permission of John Wiley & Sons, Inc.

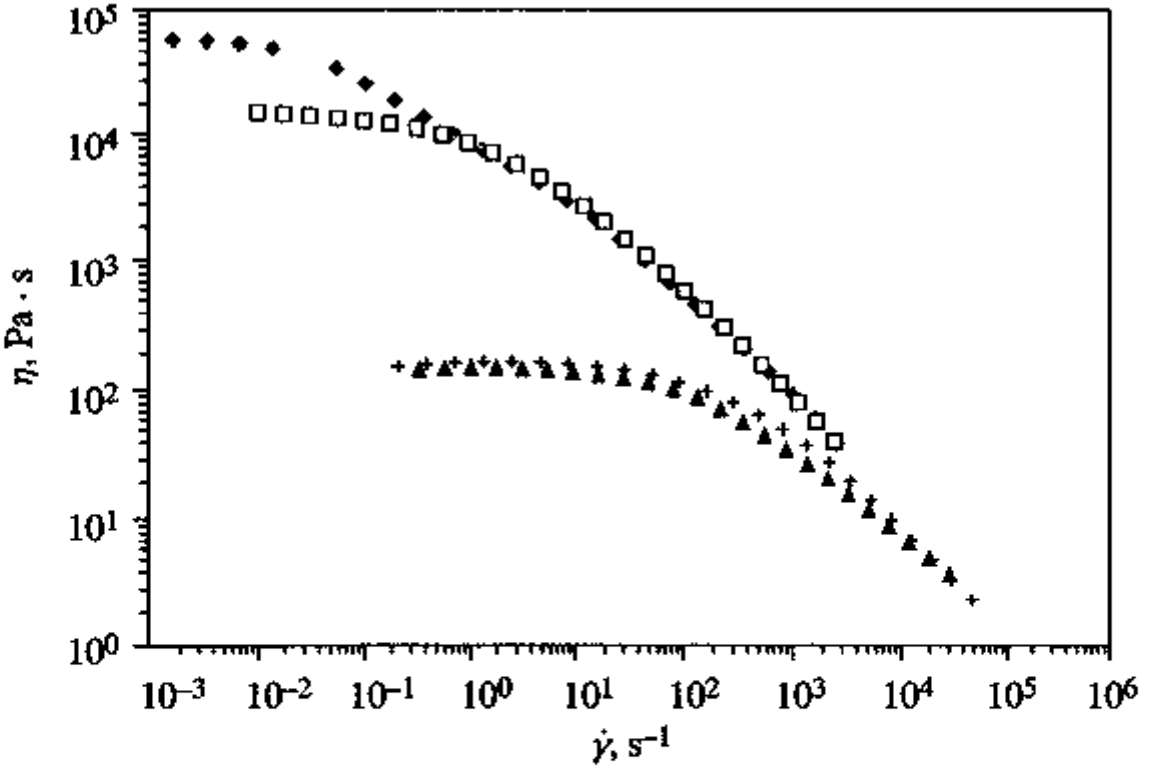

Figure 6.3 Shear viscosity η as a function of shear rate $\dot{\gamma}$ for linear and branched polydimethylsiloxanes. +, M_w=131 kg/mol, M_w/M_n=1.9, linear; △, M_w=156 kg/mol, M_w/M_n=2.8, branched; □, M_w=418 kg/mol, M_w/M_n=3.2, linear; ◇, M_w=428 kg/mol, M_w/M_n=2.9, branched; from Piau et al. [207]. *Source:* Reprinted from *Journal of Non-Newtonian Fluid Mechanics*, **30**, J. M. Piau, N. El Kissi, and B. Tremblay, "Low Reynolds number flow visualization of linear and branched silicones upstream of orifice dies," 197–232, Copyright © 1988, with permission from Elsevier Science.

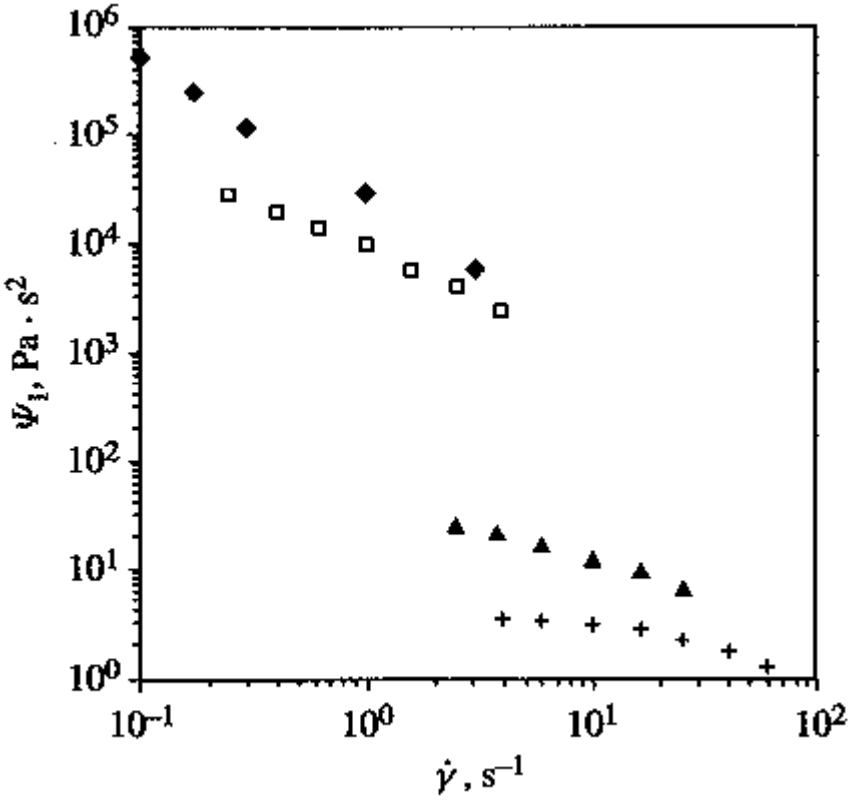

Figure 6.4 Shear first normal stress coefficient Ψ_1 as a function of shear rate $\dot{\gamma}$ for linear and branched polydimethylsiloxanes. +, $M_w = 131$ kg/mol, $M_w/M_n = 1.9$, linear; △, $M_w = 156$ kg/mol, $M_w/M_n = 2.8$, branched; □, $M_w = 418$ kg/mol, $M_w/M_n = 3.2$, linear; ◇, $M_w = 428$ kg/mol, $M_w/M_n = 2.9$, branched; from Piau et al. [207]. *Source:* Reprinted from *Journal of Non-Newtonian Fluid Mechanics*, **30**, J. M. Piau, N. El Kissi, and B. Tremblay, "Low Reynolds number flow visualization of linear and branched silicones upstream of orifice dies," 197–232, Copyright © 1988, with permission from Elsevier Science.

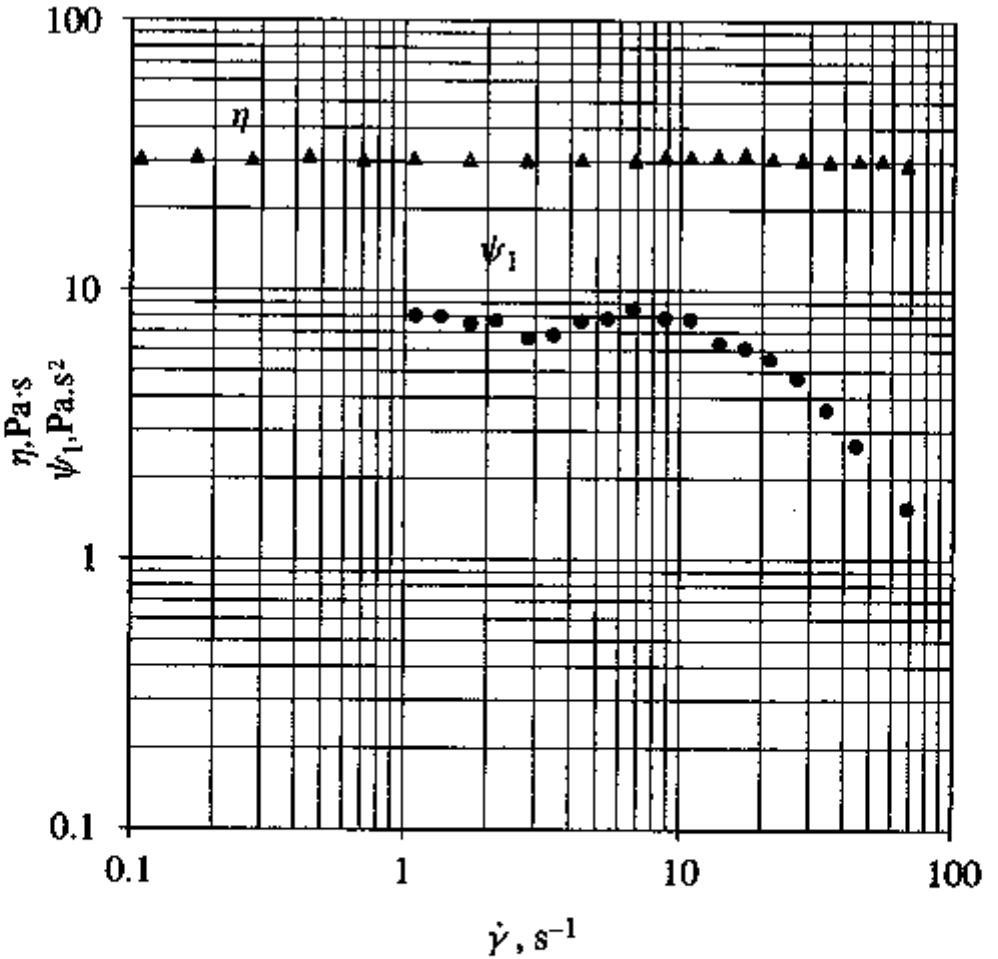

Figure 6.5 Viscosity and first normal-stress coefficient as a function of shear rate for a dilute solution of polyisobutylene in a viscous solvent, a mixture of polybutene and kerosene; from Binnington and Boger [24]. This is a Boger fluid; note that the viscosity is constant, but the fluid is clearly not Newtonian since $\Psi_1 \neq 0$. *Source:* From the *Journal of Rheology,* Copyright © 1985, The Society of Rheology. Reprinted by permission.

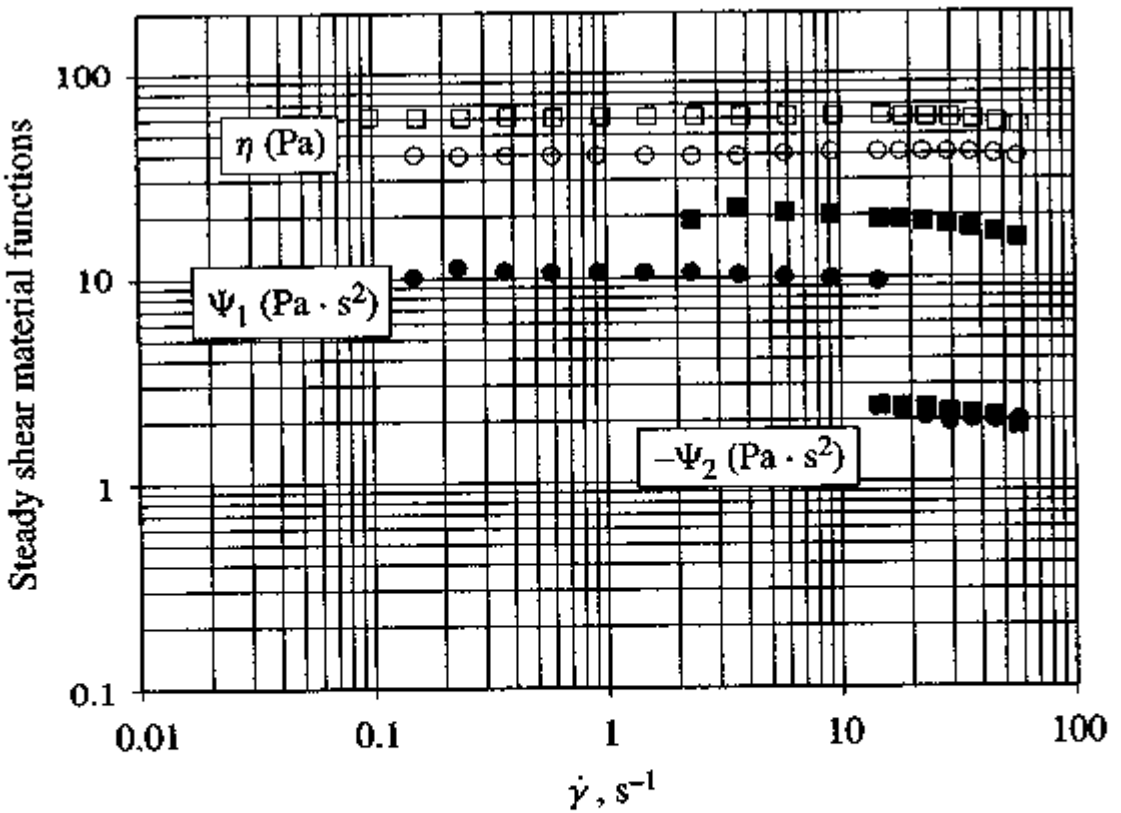

Figure 6.6 All three shear-flow material functions (η, Ψ_1, Ψ_2) as a function of shear rate for two polystyrene solutions; from Magda et al. [163]. ○, 28% polystyrene in dioctylpthalate (DOP); □, 28% polystyrene in tricresylphosphate (TCP). The polystyrene in these solutions is broadly distributed with $M_w = 47$ kg/mol. *Source:* Reprinted with permission, "Rheology, flow instabilities, and shear-induced diffusion in polystyrene solutions," J. J. Magda, C. S. Lee, S. J. Muller, and R. G. Larson, *Macromolecules*, **26**, 1696–1706 (1993). Copyright © 1993, American Chemical Society.

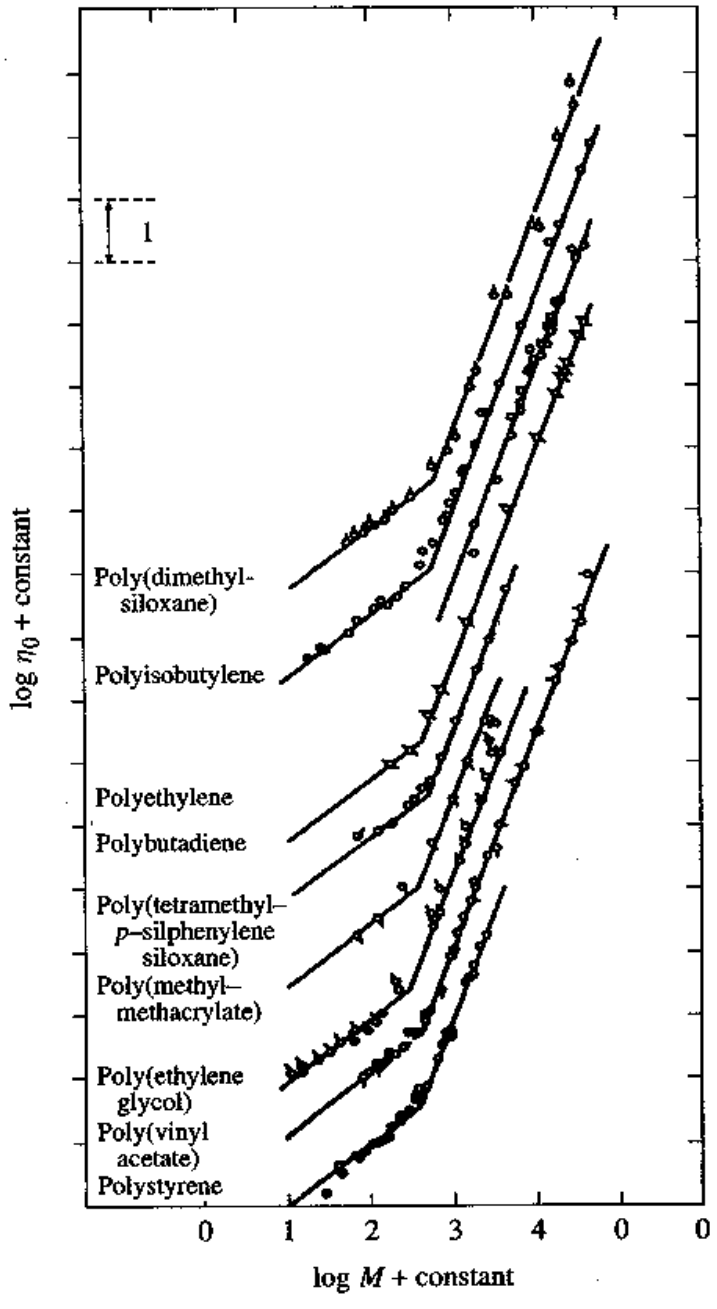

Figure 6.12 Effect of molecular weight on the measured zero-shear viscosity for a variety of polymers; from Berry and Fox [21]. Below a critical molecular weight M_c, $\eta_0 \propto M^1$; at higher molecular weights $\eta_0 \propto M^{3.4-3.5}$. *Source:* From "The viscosity of polymers and their concentrated solutions," G. C. Berry and T. G Fox, *Advances in Polymer Science*, **5**, 261–357 (1968), Figure 1. Copyright © 1968, Springer-Verlag.

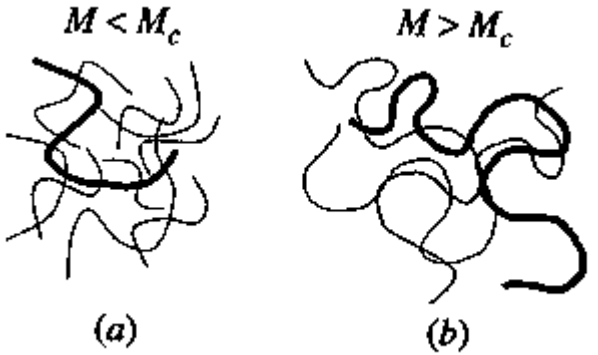

Figure 6.13 Schematic of (*a*) unentangled and (*b*) entangled polymers. Unentangled polymers are able to rapidly relax interactions with neighboring molecules. Entangled polymers form knots and are slowed down in their ability to relax interactions with their neighbors.

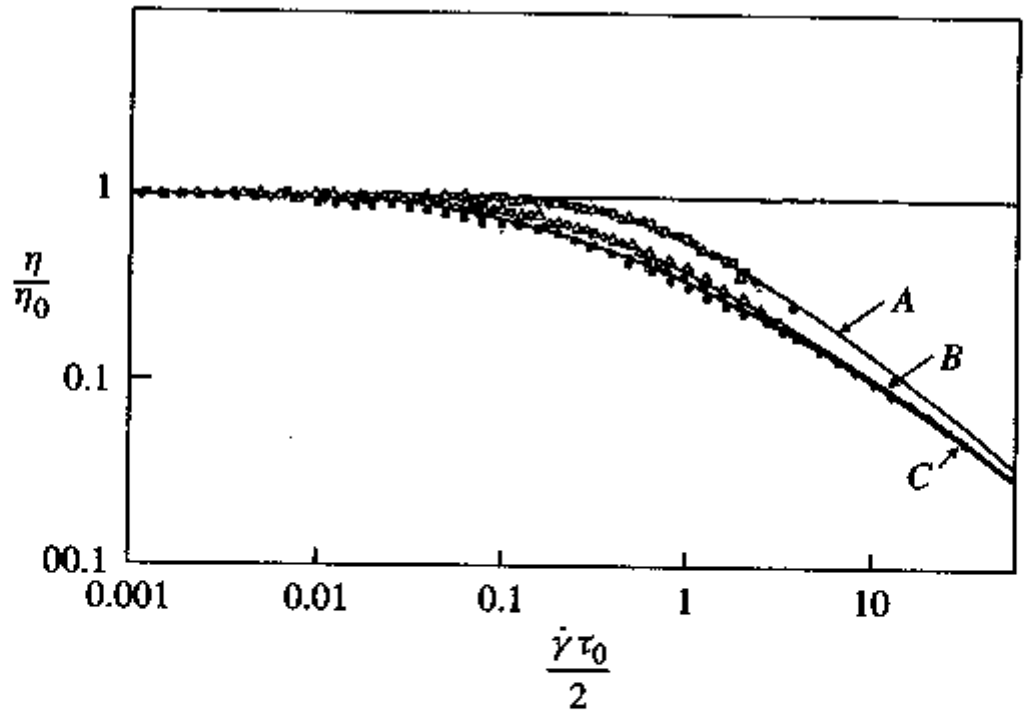

Figure 6.14 Effect of molecular weight distribution on viscosity; from Uy and Graessley [250a]. Shown are viscosity versus shear-rate master curves for poly(vinyl acetate) concentrated solutions in diethyl phthalate. Polymers of different M_w values were shifted empirically using the zero-shear viscosity η_0 and a time constant $\tau_0/2$ to produce the master curves for comparison. The different curves represent samples with different molecular weight distributions: *A*—$M_w/M_n = 1.09$; *B*—$M_w/M_n = 2.0$; *C*—branched. *Source:* Reprinted with permission, "Viscosity and normal stresses in poly(vinyl acetate) systems," W. C. Uy and W. W. Graessley, *Macromolecules*, **4**, 458–463 (1971). Copyright © 1971, American Chemical Society.

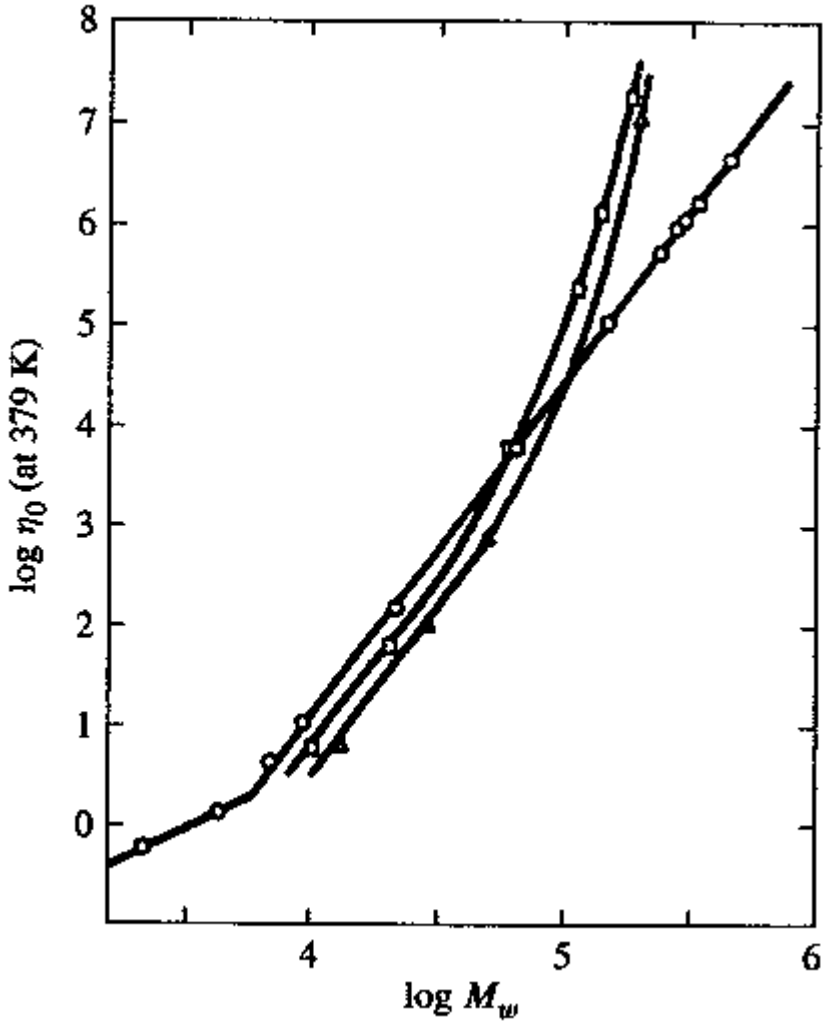

Figure 6.17 Effect of branching on zero-shear viscosity η_0, that is, at low shear rates; from Kraus and Gruver [131]. Curves are for ○ linear, □ three-armed star-branched (linear with one long side chain), and △ four-armed star-branched polybutadienes at 379 K. At lower molecular weights the branched polymers have lower η_0; at very high molecular weights, however, the viscosity of the branched polymers greatly exceeds that of the linear polymer. *Source:* From "Rheological properties of multichain polybutadienes," by G. Kraus and J. T. Gruver, *Journal of Polymer Science, Part A*, Copyright © 1965 by John Wiley & Sons, Inc. Reprinted by permission of John Wiley & Sons, Inc.

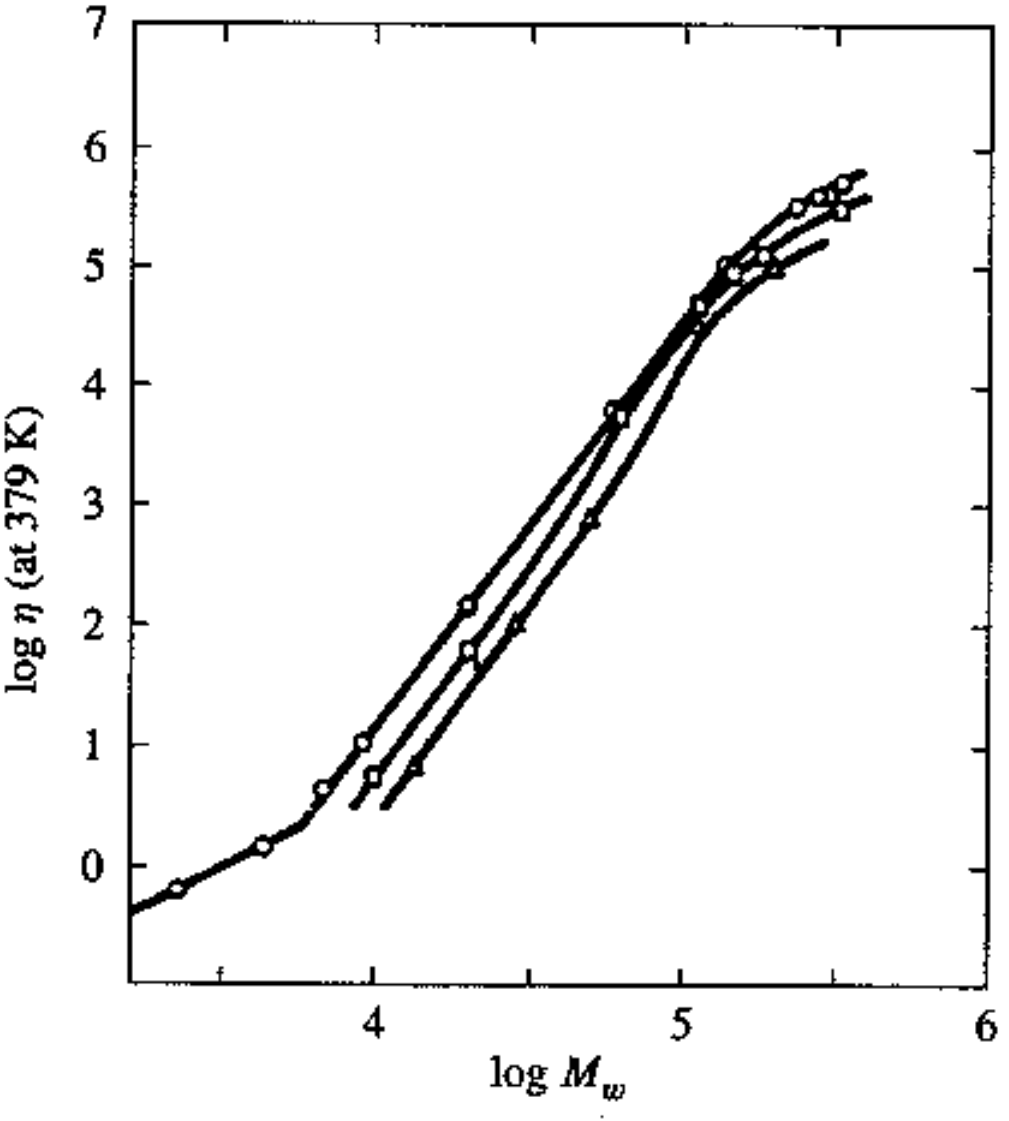

Figure 6.19 Effect of branching on viscosity at $\dot{\gamma} = 20\ s^{-1}$; from Kraus and Gruver [131]. Symbols are defined in Figure 6.17. $\eta(\dot{\gamma} = 20\ s^{-1})$ is lower for branched polybutadienes than for linear polybutadienes of the same molecular weight. *Source:* From "Rheological properties of multichain polybutadienes," by G. Kraus and J. T. Gruver, *Journal of Polymer Science, Part A*, Copyright © 1965 by John Wiley & Sons, Inc. Reprinted by permission of John Wiley & Sons, Inc.

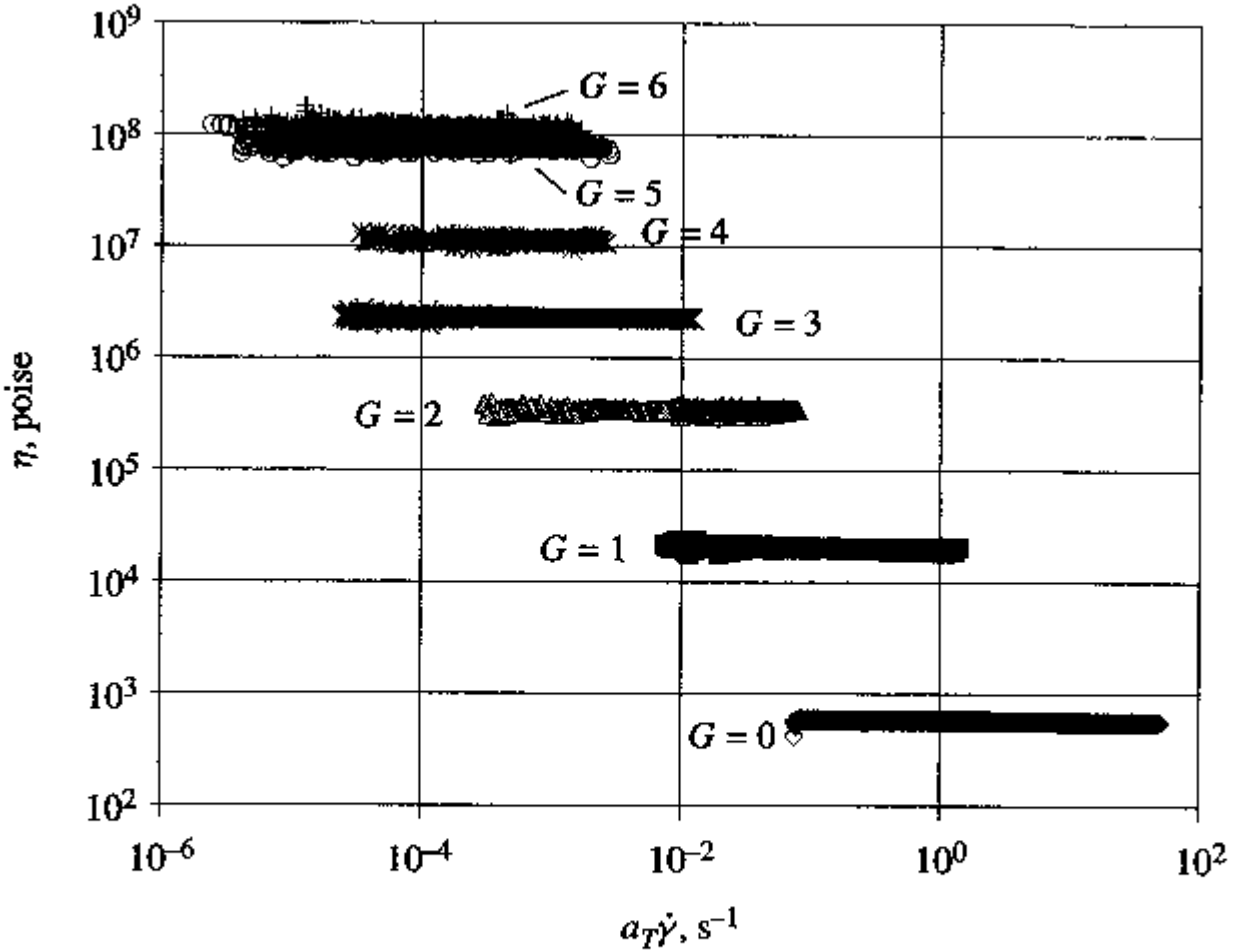

Figure 6.20 Steady shear viscosity of generations (G) 0 through 6 ethylenediamine (EDA)-core, poly(amidoamine) (PAMAM)-bulk dendrimers at 70°C; from Uppuluri [248]. Each generation represents an additional growth cycle of the dendrimer, that is, increasing molecular weight.

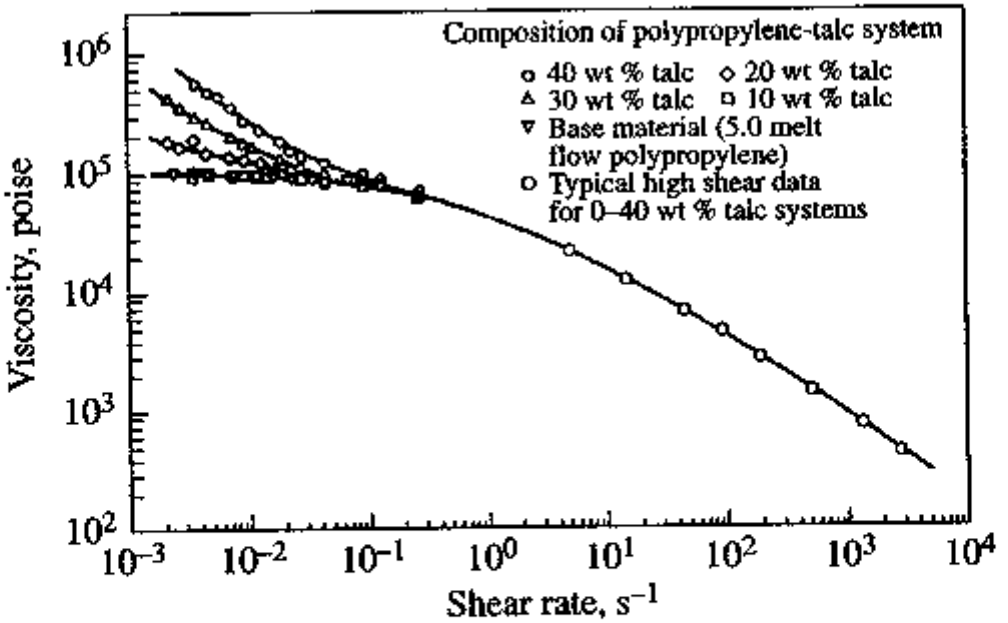

Figure 6.21 Viscosity versus shear rate at 200°C for talc-filled polypropylene; from Chapman and Lee [40]. Data at low rates were taken in a cone-and-plate rheometer; high-rate data were taken in a capillary rheometer. *Source:* From *SPE Journal,* Copyright © 1970, Society of Plastics Engineers. Reprinted by permission.

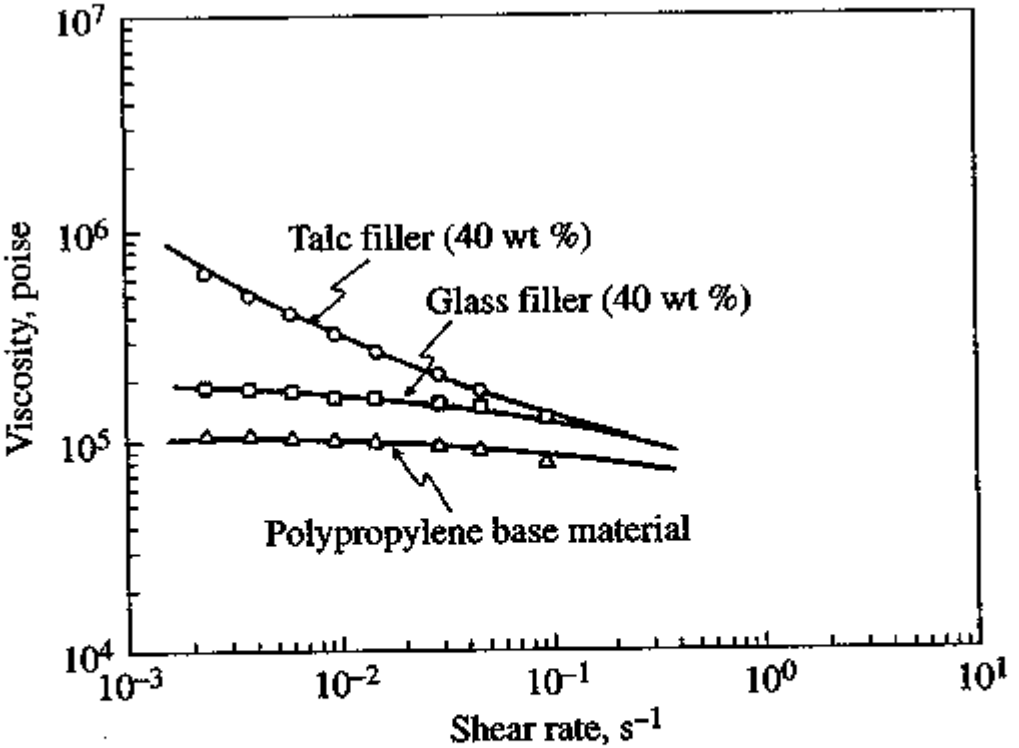

Figure 6.22 Viscosity versus shear rate for polypropylene and for polypropylene mixed with inert glass filler and interacting talc filler; from Chapman and Lee [40]. Although the absence of specific interactions reduces the viscosity of the glass-filled compared to the talc-filled polypropylene, the viscosity of the glass-filled system is still greater than that of the neat polymer. *Source:* From *SPE Journal,* Copyright © 1970, Society of Plastics Engineers. Reprinted by permission.

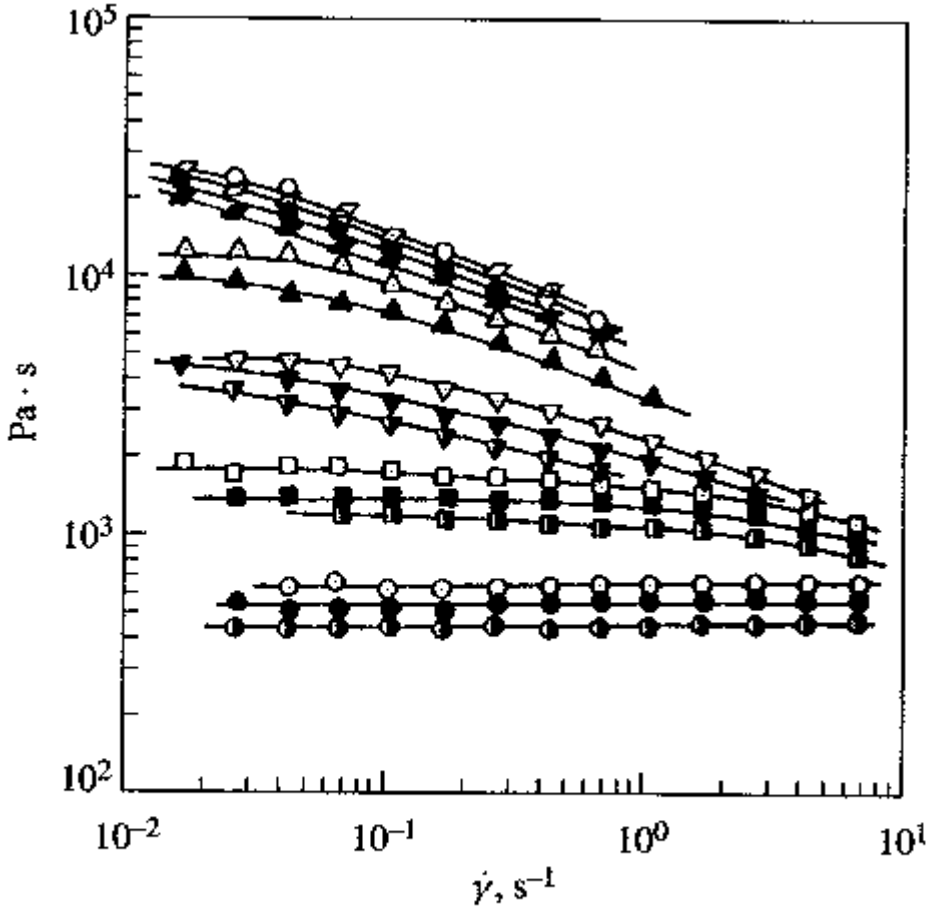

Figure 6.23 Viscosity η versus shear rate $\dot{\gamma}$ for blends of nylon and a branched polyolefin at various temperatures; from Chuang and Han [46]. Various blend compositions are shown. The nylon wt % of the blends varies as follows: ○, 100; □, 80; ▽, 60; ⬭, 40; ◇, 20; △, 0. Temperatures (°C) are indicated by the shading of the symbols: left half filled, 220; open, 230; filled in, 240; right half filled, 250. *Source:* Reprinted with permission, "Rheological behavior of blends of nylon with a chemically modified polyolefin," H.-K Chuang and C. D. Han, *Advances in Chemistry: Polymer Blends and Composites in Multiphase Systems*, **206**, 171–183 (1984). Copyright © 1984, American Chemical Society.

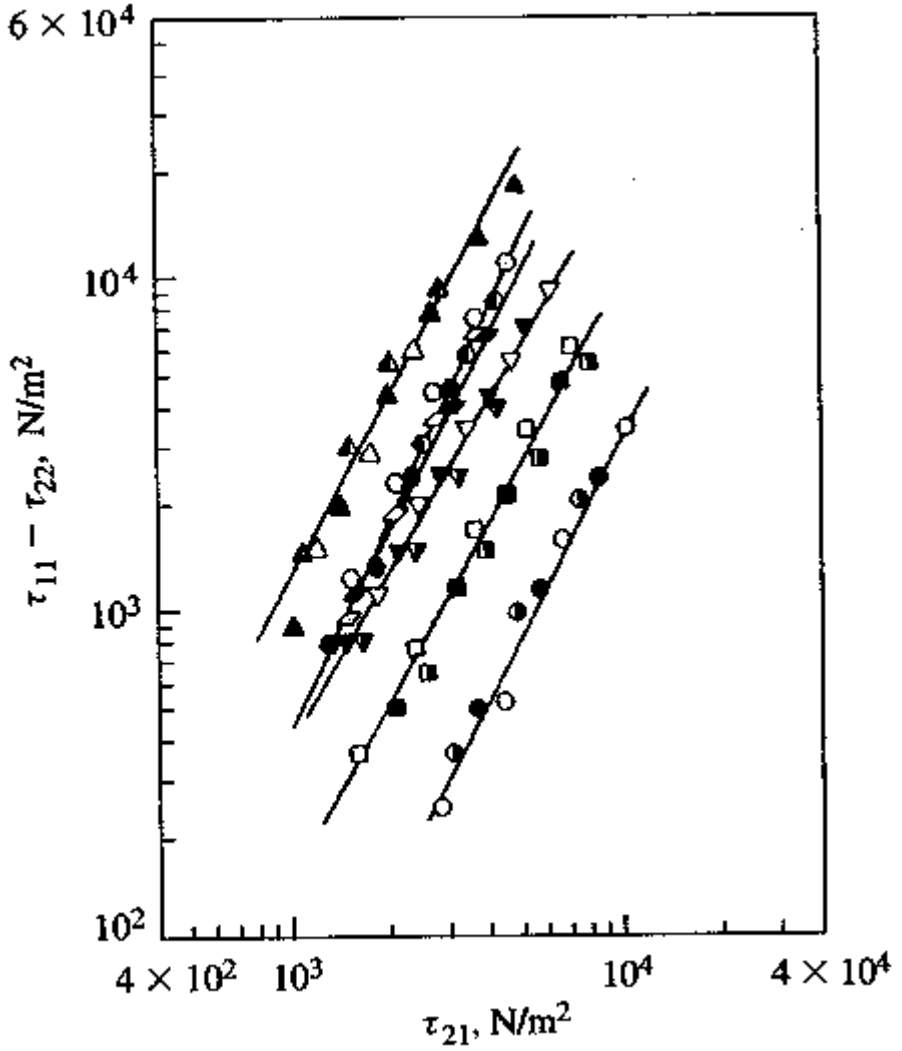

Figure 6.24 First normal-stress difference $N_1 = \tau_{11} - \tau_{22}$ versus shear stress τ_{21} for blends of nylon and a branched polyolefin at various temperatures; from Chuang and Han [46]. Various blend compositions are shown. The symbols are defined in Figure 6.23. *Source:* Reprinted with permission, "Rheological behavior of blends of nylon with a chemically modified polyolefin," H.-K Chuang and C. D. Han, *Advances in Chemistry: Polymer Blends and Composites in Multiphase Systems*, **206**,171–183 (1984). Copyright © 1984, American Chemical Society.

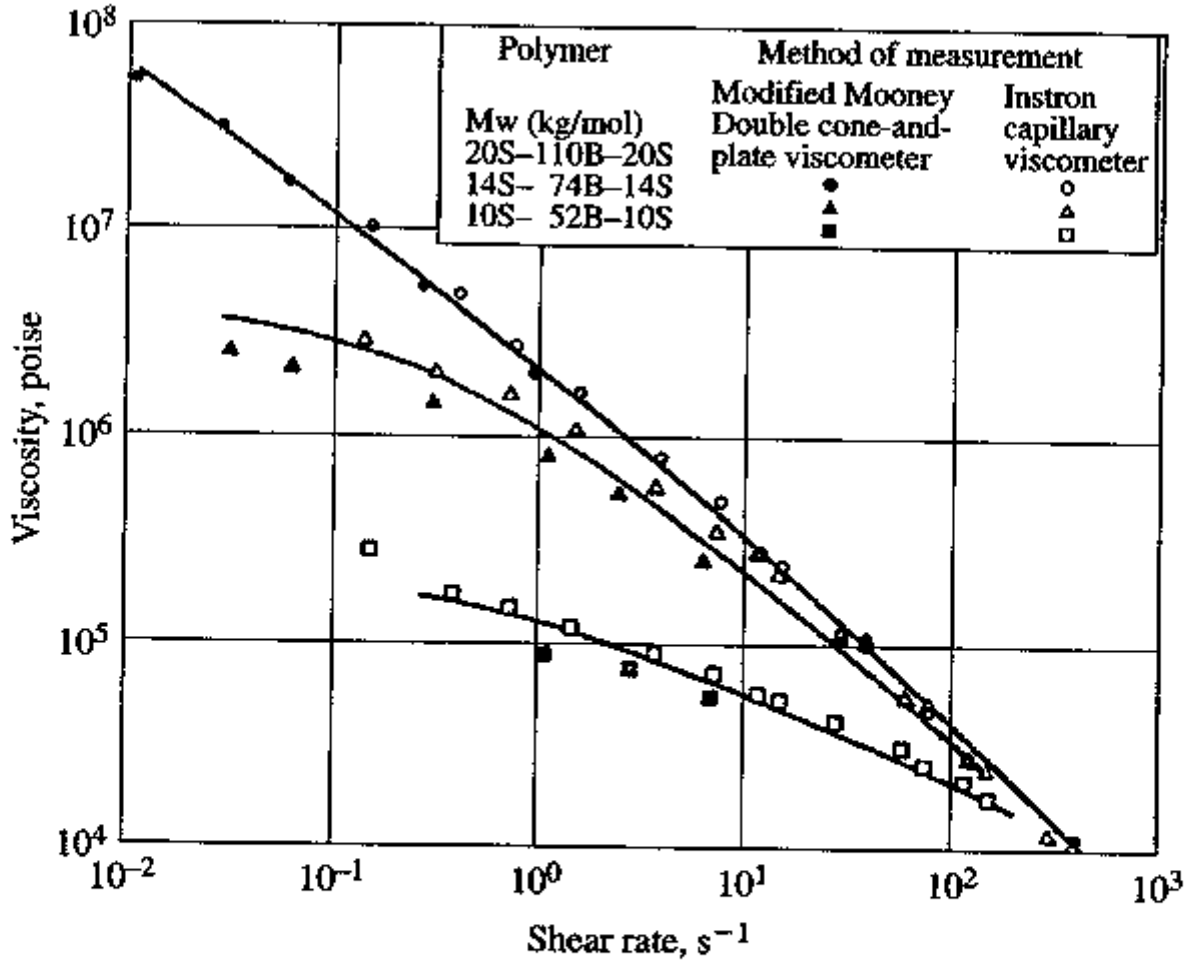

Figure 6.25 Steady shear viscosities versus shear rate of three (*b*)polystyrene–(*b*)polybutadiene–(*b*)polystyrene (SBS) triblock copolymers at 175°C; from Holden et al. [111]. Block molecular weights of each copolymer are also listed. *Source:* From "Thermoplastic elastomers," by G. Holden, E. T. Bishop and N. R. Legge, *Journal of Polymer Science, Part C*, Copyright © 1969 by John Wiley & Sons, Inc. Reprinted by permission of John Wiley & Sons, Inc.

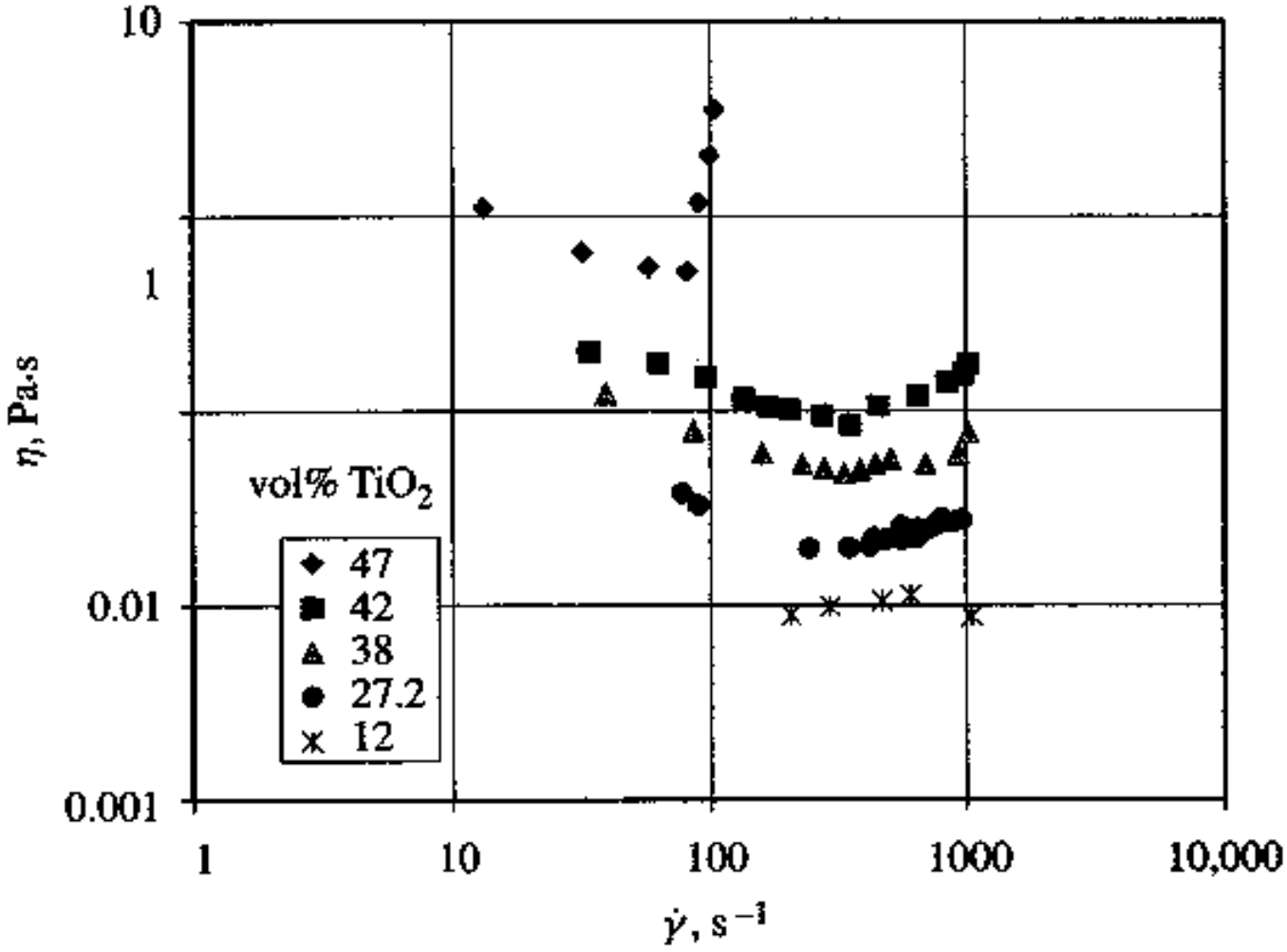

Figure 6.27 Viscosity versus shear rate for five suspensions of TiO_2 in water; recalculated and replotted from Metzner and Whitlock [178]. The diameters of the TiO_2 particles were between 0.2 and 1 μm, and the data were taken on a Couette (cup-and-bob) rheometer. *Source:* From the *Transactions of the Society of Rheology,* Copyright © 1958, The Society of Rheology. Reprinted by permission.

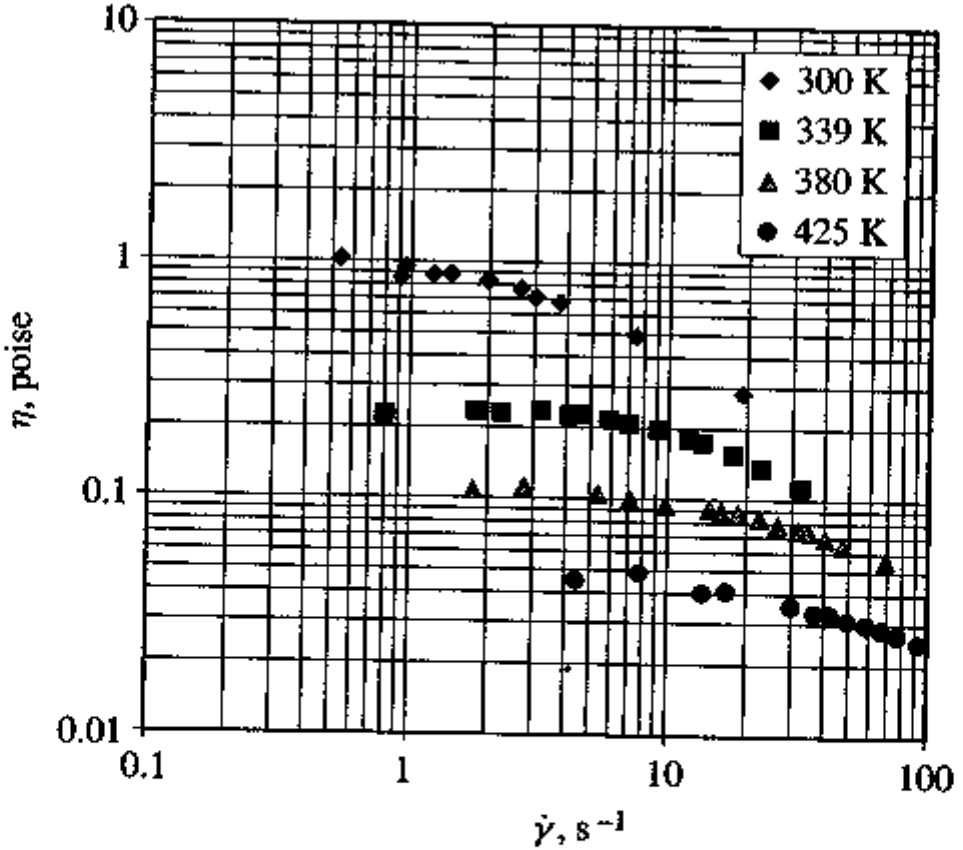

Figure 6.28 Viscosity versus shear rate at four different temperatures for a polybutadiene melt. Raw capillary data from Gruver and Kraus [102] corrected for nonparabolic velocity profile (Rabinowitsch correction; see Chapter 10) and plotted. $M_w = 145$ kg/mol, $M_w/M_n = 1.1$. From "Rheological properties of polybutadienes prepared by n-butyllithium initiation," by J. T. Gruver and G. Kraus, *Journal of Polymer Science, Part A*, Copyright © 1964 by John Wiley & Sons, Inc. Reprinted by permission of John Wiley & Sons, Inc.

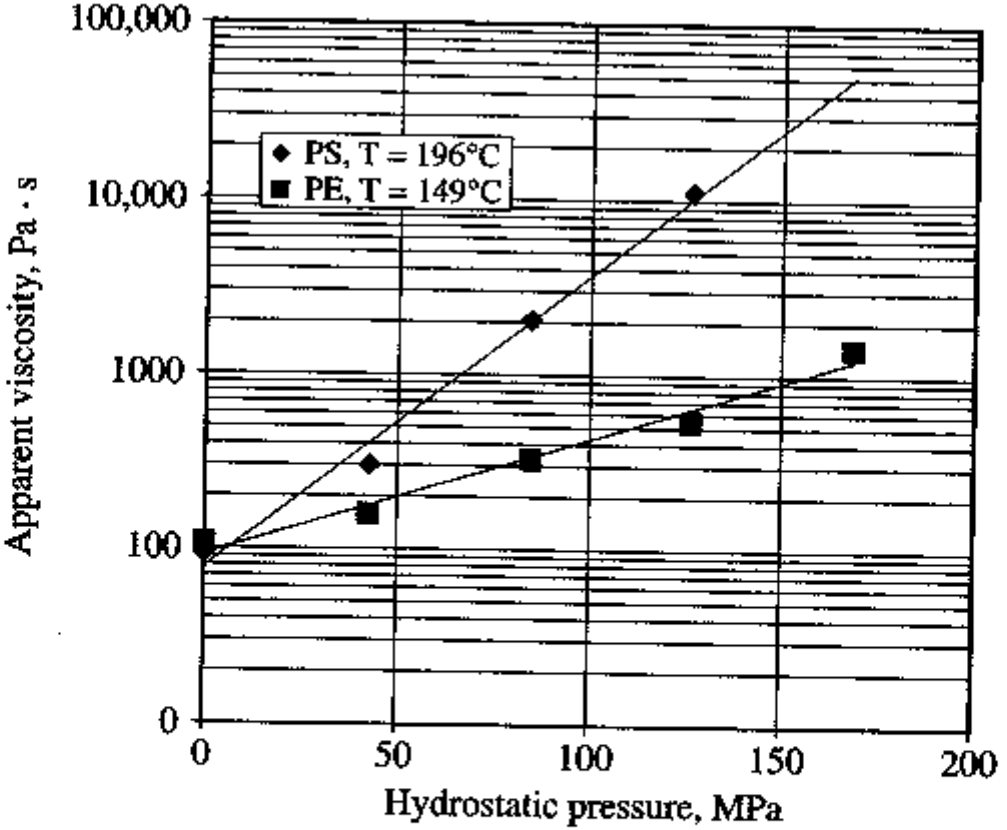

Figure 6.29 Apparent viscosity of polystyrene and branched polyethylene as a function of pressure; replotted from Maxwell and Jung [172]. Use of the term "apparent viscosity" reflects that the Rabinowitsch correction has not been applied; see Chapter 10. *Source:* Reprinted from *Modern Plastics*, March, 1957, pp. 174–182, 276, a publication of the McGraw-Hill Companies, Inc.

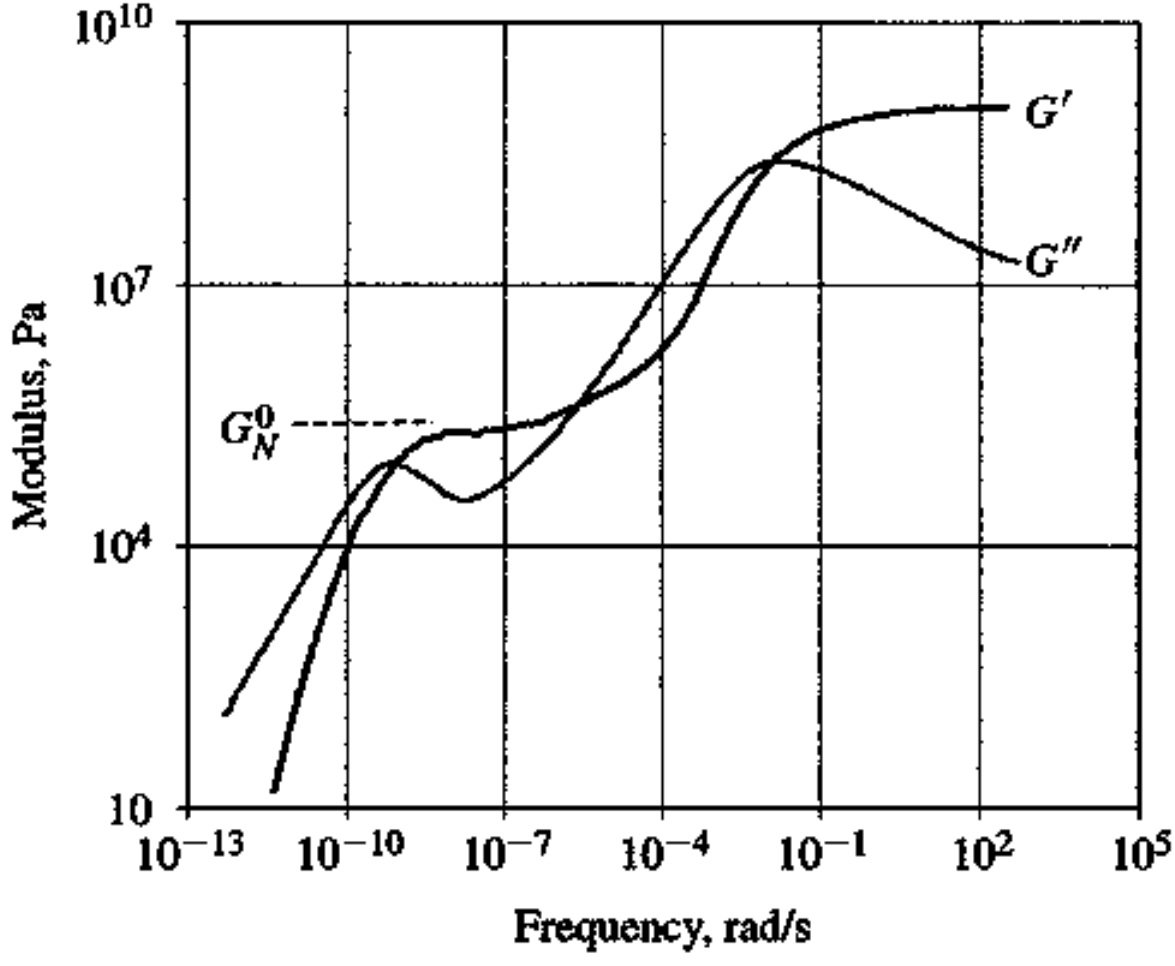

Figure 6.30 Master curve of the material functions $G'(\omega)$ and $G''(\omega)$ for an atactic linear polystyrene; data taken by D. J. Plazek and V. M. O'Rourke as plotted in Ferry [75]. $M_w = 600$ kg/mol, narrow molecular-weight distribution. The reference temperature is 100°C. *Source:* From *Viscoelastic Properties of Polymers*, J. D. Ferry, Copyright © 1980 by John Wiley & Sons. Reprinted by permission of John Wiley & Sons, Inc.

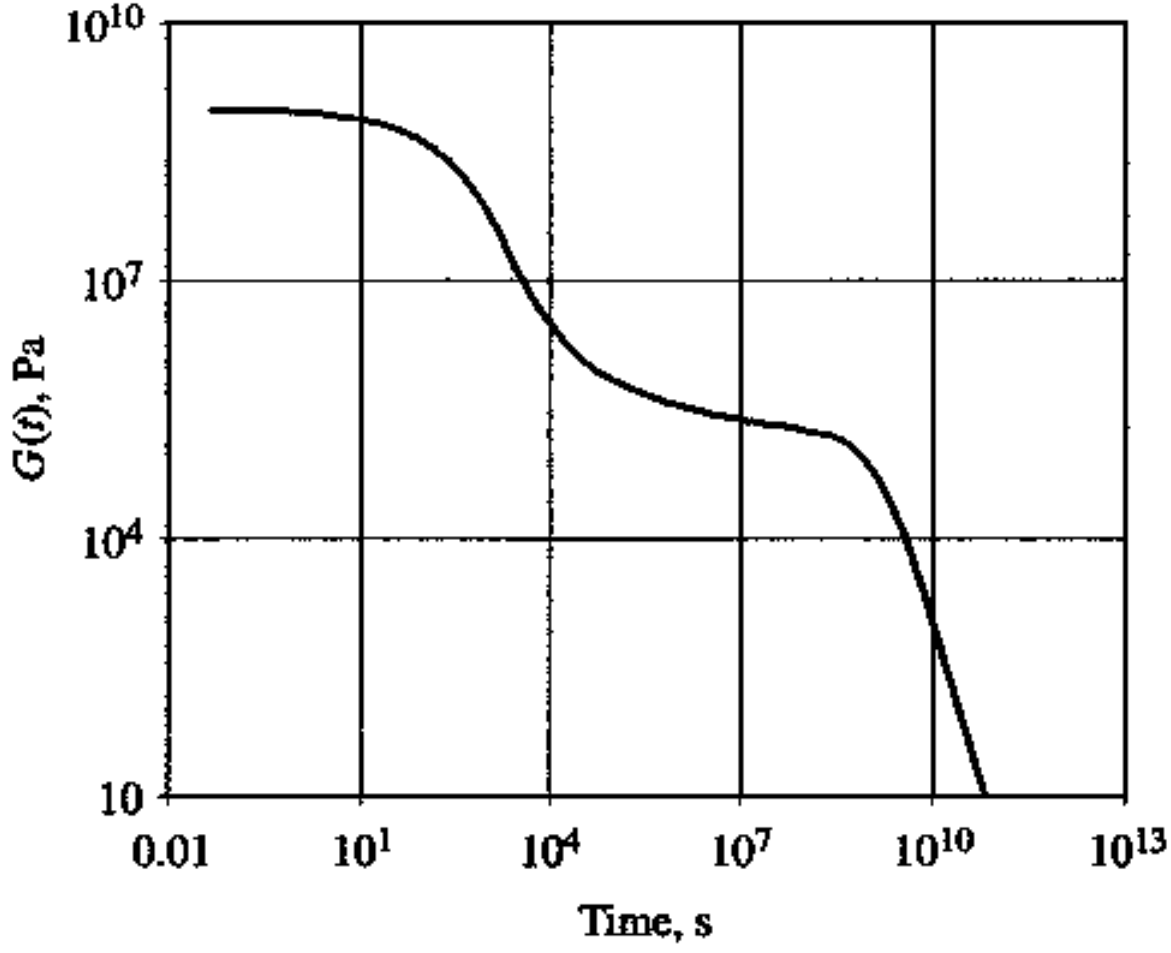

Figure 6.31 Master curve of the material function $G(t)$, the relaxation modulus, for an atactic linear polystyrene; calculated from the G' and G'' data in Figure 6.30 calculated by Ferry [75] from the data taken by D. J. Plazek and V. M. O'Rourke. The reference temperature is 100°C. *Source:* From *Viscoelastic Properties of Polymers*, J. D. Ferry, Copyright © 1980 by John Wiley & Sons. Reprinted by permission of John Wiley & Sons, Inc.

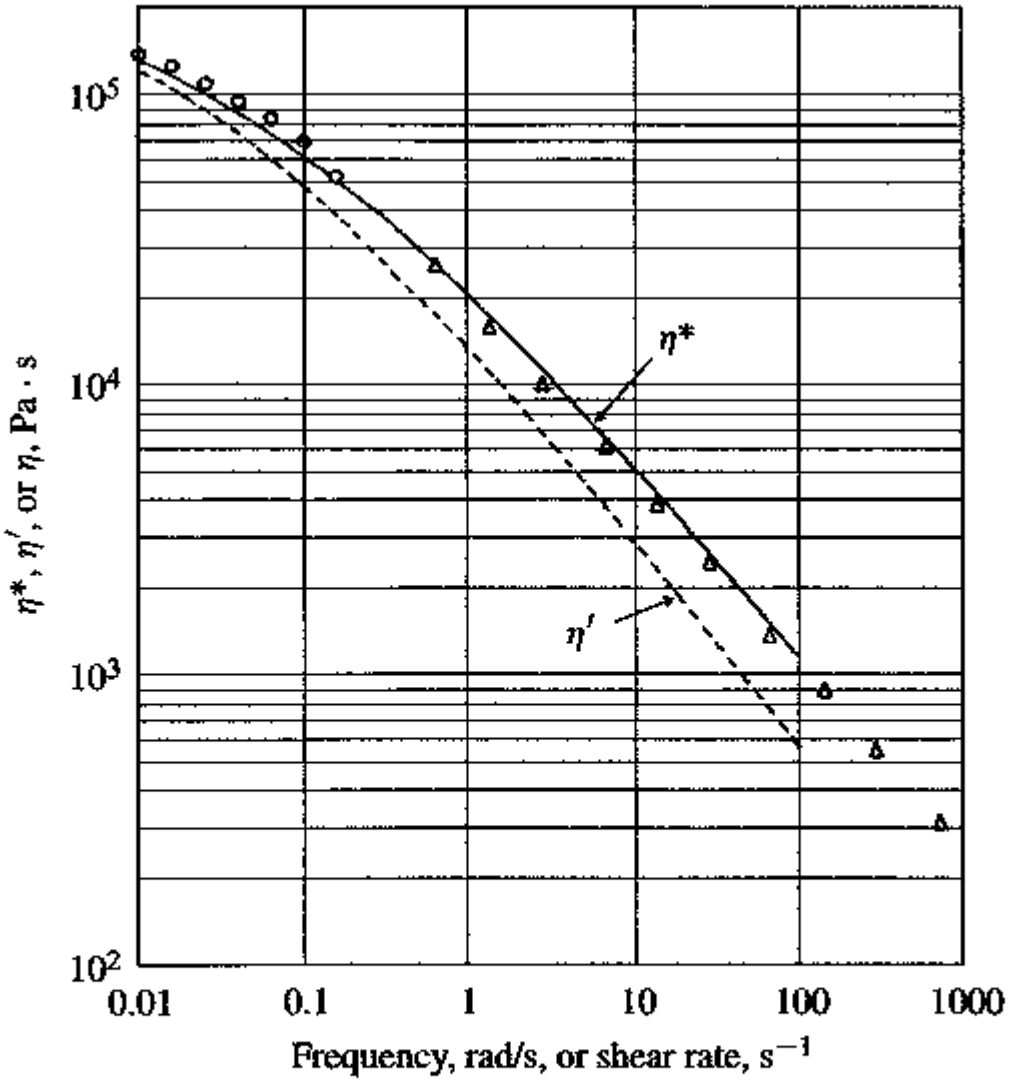

Figure 6.32 Dynamic (η', η^*) and steady shear (η) viscosities versus frequency and shear rate, respectively, for a low-density polyethylene (LDPE) at 175°C; from Venkatraman et al. [251]. ○, data taken in a cone-and-plate rheometer; △, corrected capillary data. *Source:* From *Polymer Engineering and Science,* Copyright © 1990, Society of Plastics Engineers. Reprinted by permission.

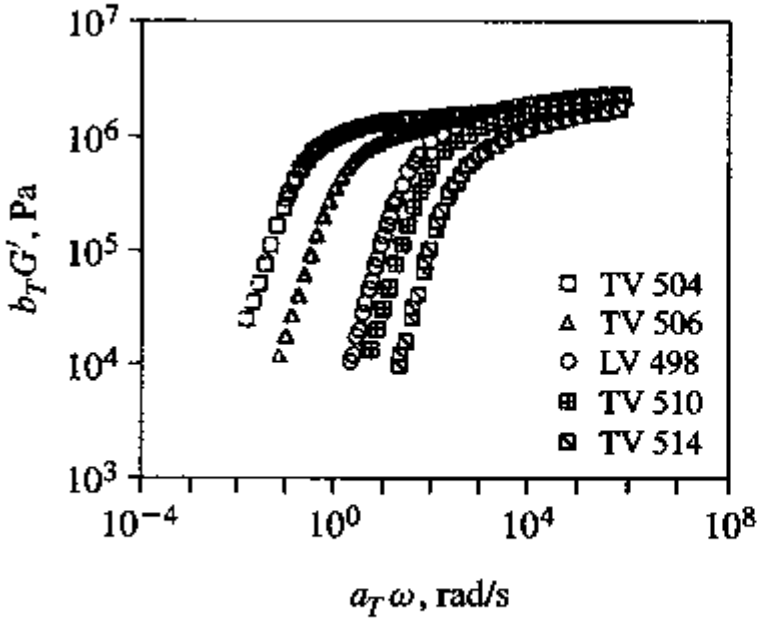

Figure 6.33 Master curves of storage modulus $b_T G'$ versus $a_T \omega$ for narrow-molecular-weight-distribution polybutadienes of various molecular weights; from Palade et al. [201]. b_T is the vertical shift factor, $b_T \equiv T_{\text{ref}} \rho_{\text{ref}} / T\rho$. Master curves were obtained from time–temperature superposition. $T_{\text{ref}} = 25°\text{C}$, M_w (kg/mol): TV504 = 464, TV506 = 229, LV498 = 85.8, TV510 = 70.6, TV514 = 51.3. *Source:* Reprinted with permission, "Time–temperature superposition and linear viscoelasticity of polybutadienes," L. I. Palade, V. Verney, and P. Attane, *Macromolecules*, **28**, 7051–7057 (1995). Copyright © 1995, American Chemical Society.

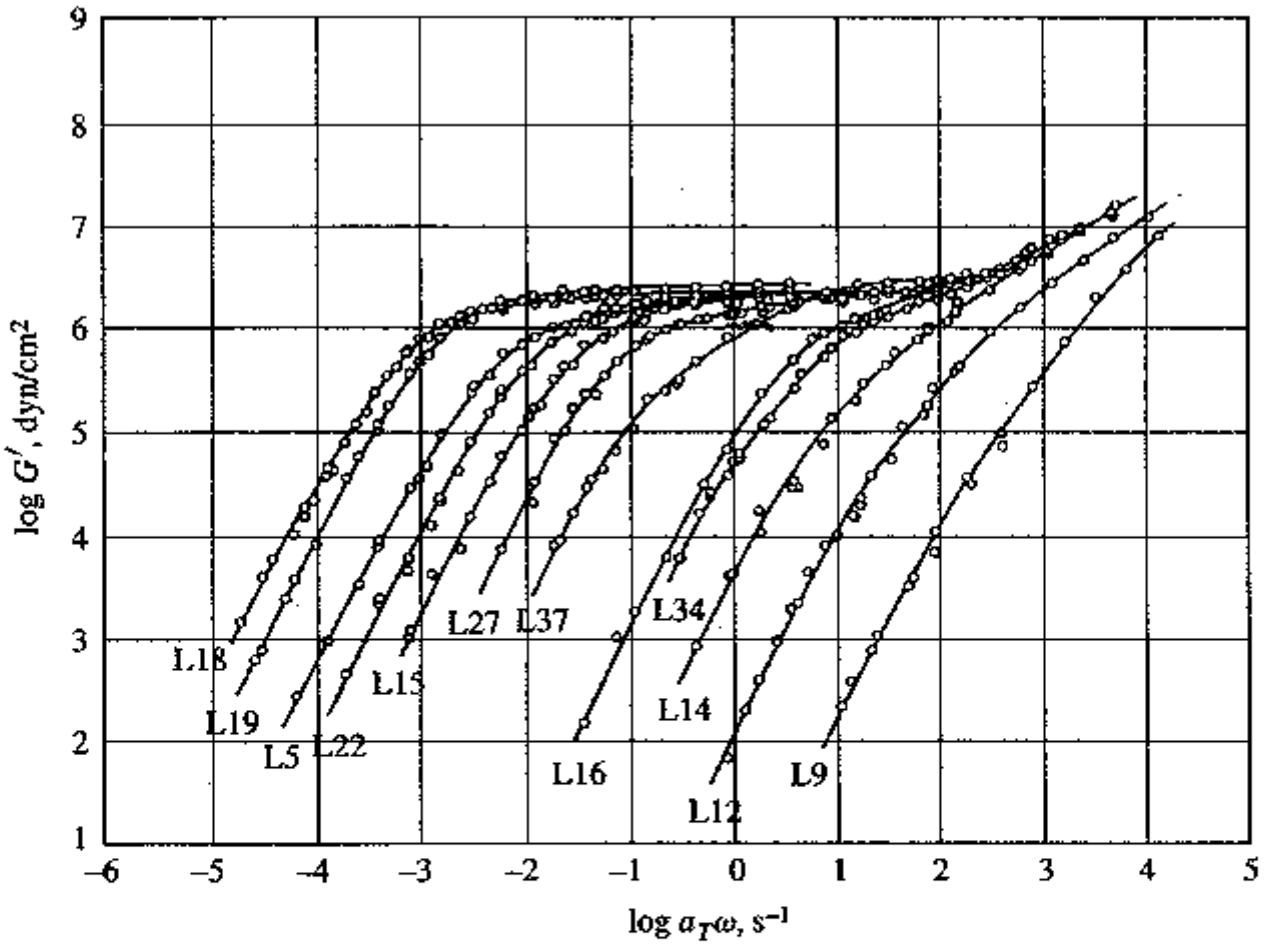

Figure 6.34 Master curves of storage modulus G' versus $a_T\omega$ for narrow-molecular-weight-distribution polystyrenes of various molecular weights; from Onogi et al. [196]. Master curves were obtained from time–temperature superposition. T_{ref} = 160°C, M_w (kg/mol): L18 = 581, L19 = 513, L5 = 351, L22 = 275, L15 = 215, L27 = 167, L37 = 113, L16 = 58.7, L34 = 46.9, L14 = 28.9, L12 = 14.8, L9 = 8.9. *Source:* Reprinted with permission, "Rheological properties of anionic polystyrenes. I. Dynamic viscoelasticity of narrow-distribution polystyrenes," Onogi, S., T. Masuda, and K. Kitagawa, *Macromolecules*, **3**, 109–116 (1970). Copyright © 1970, American Chemical Society.

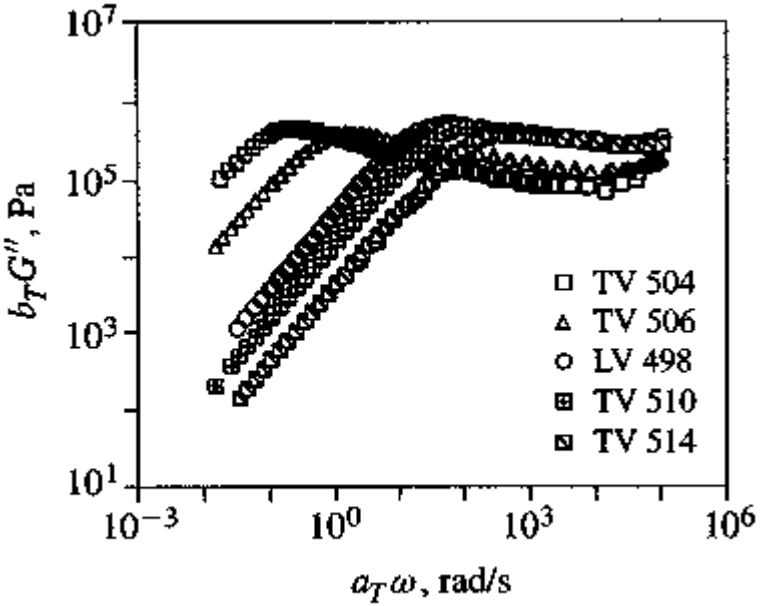

Figure 6.35 Master curves of loss modulus G'' versus $a_T\omega$ for narrow-molecular-weight-distribution polybutadienes of various molecular weights; from Palade et al. [201]. Master curves were obtained from time–temperature superposition. $T_{\text{ref}} = 25°\text{C}$; M_w listed in Figure 6.33. *Source:* Reprinted with permission, "Time–temperature superposition and linear viscoelasticity of polybutadienes," L. I. Palade, V. Verney, and P. Attane, *Macromolecules*, **28**, 7051–7057 (1995). Copyright © 1995, American Chemical Society.

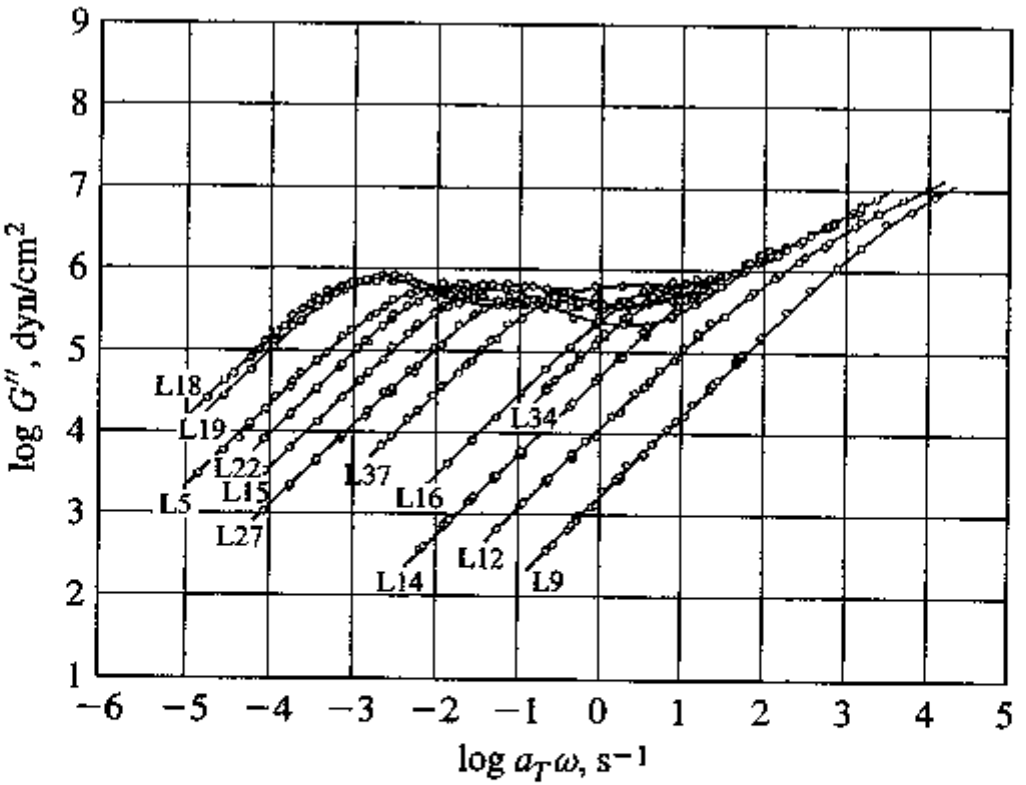

Figure 6.36 Master curves of loss modulus G'' versus $a_T\omega$ for narrow-molecular-weight-distribution polystyrenes of various molecular weights; from Onogi et al. [196]. Master curves were obtained from time–temperature superposition. $T_{ref} = 160°C$; M_w listed in Figure 6.34. *Source:* Reprinted with permission, "Rheological properties of anionic polystyrenes. I. Dynamic viscoelasticity of narrow-distribution polystyrenes," Onogi, S., T. Masuda, and K. Kitagawa, *Macromolecules*, **3**, 109–116 (1970). Copyright © 1970, American Chemical Society.

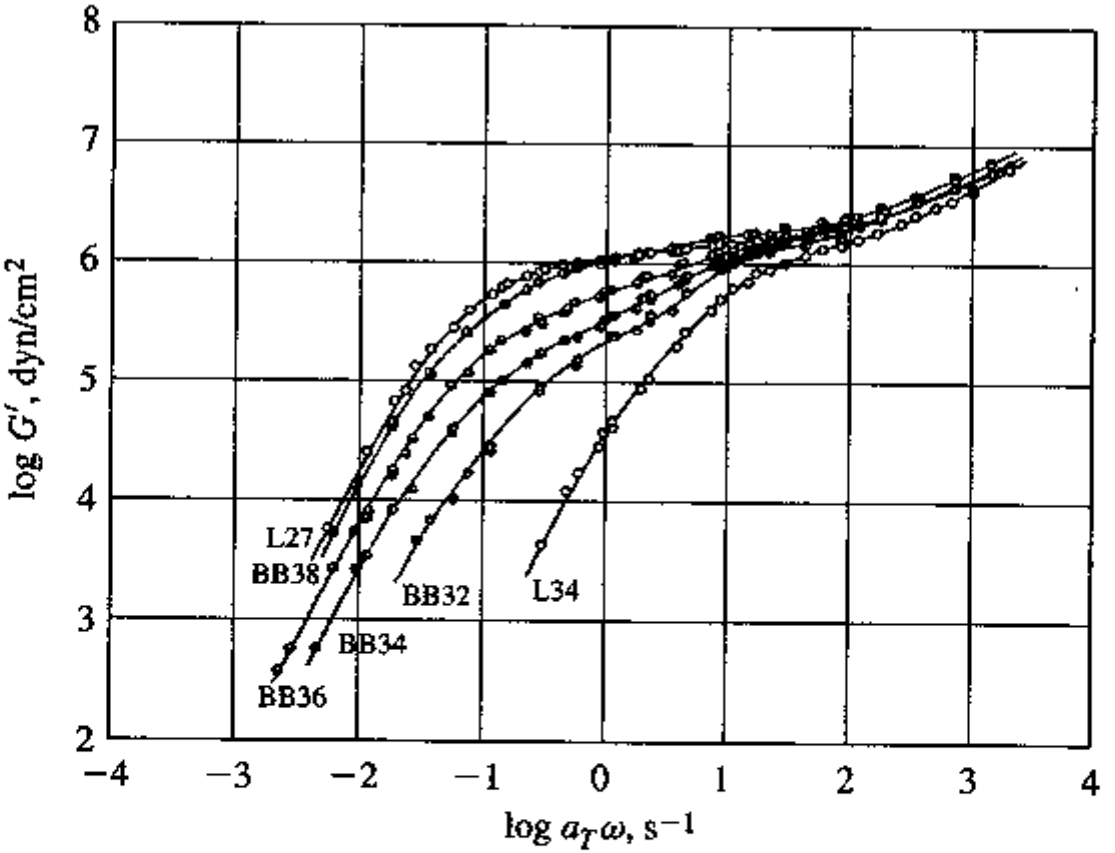

Figure 6.37 Master curves of storage modulus G' versus $a_T\omega$ for narrow-molecular-weight-distribution polystyrene melts and blends; from Masuda et al. [168]. $T_{ref} = 160°C$. Mixtures of two molecular weights: L34 = 46.9 kg/mol and L27 = 167 kg/mol. Binary blends have compositions as follows: BB38 = 80 wt % L27, BB36 = 60 wt % L27, BB34 = 40 wt % L27, and BB32 = 20 wt % L27. *Source:* Reprinted with permission, "Rheological properties of anionic polystyrenes. II. Dynamic viscoelasticity of blends of narrow-distribution polystyrenes," T. Masuda, K. Kitagawa, T. Inoue, and S. Onogi, *Macromolecules*, 3, 116–125 (1970). Copyright © 1970, American Chemical Society.

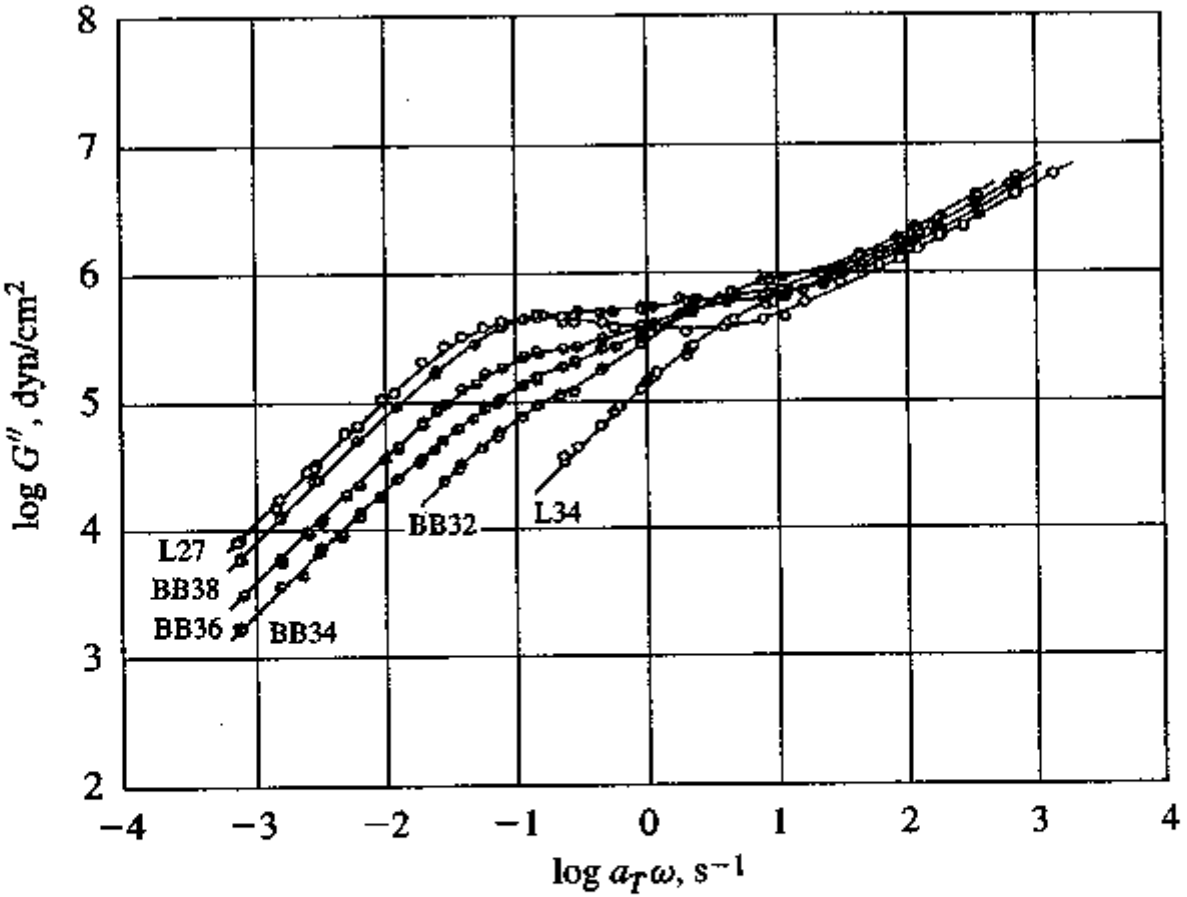

Figure 6.38 Master curves of loss modulus G'' versus $a_T\omega$ for narrow-molecular-weight-distribution polystyrene melts and blends from Masuda et al. [168]. $T_{ref} = 160°C$. Samples are identified in Figure 6.37. *Source:* Reprinted with permission, "Rheological properties of anionic polystyrenes. II. Dynamic viscoelasticity of blends of narrow-distribution polystyrenes," T. Masuda, K. Kitagawa, T. Inoue, and S. Onogi, *Macromolecules*, 3, 116–125 (1970). Copyright © 1970, American Chemical Society.

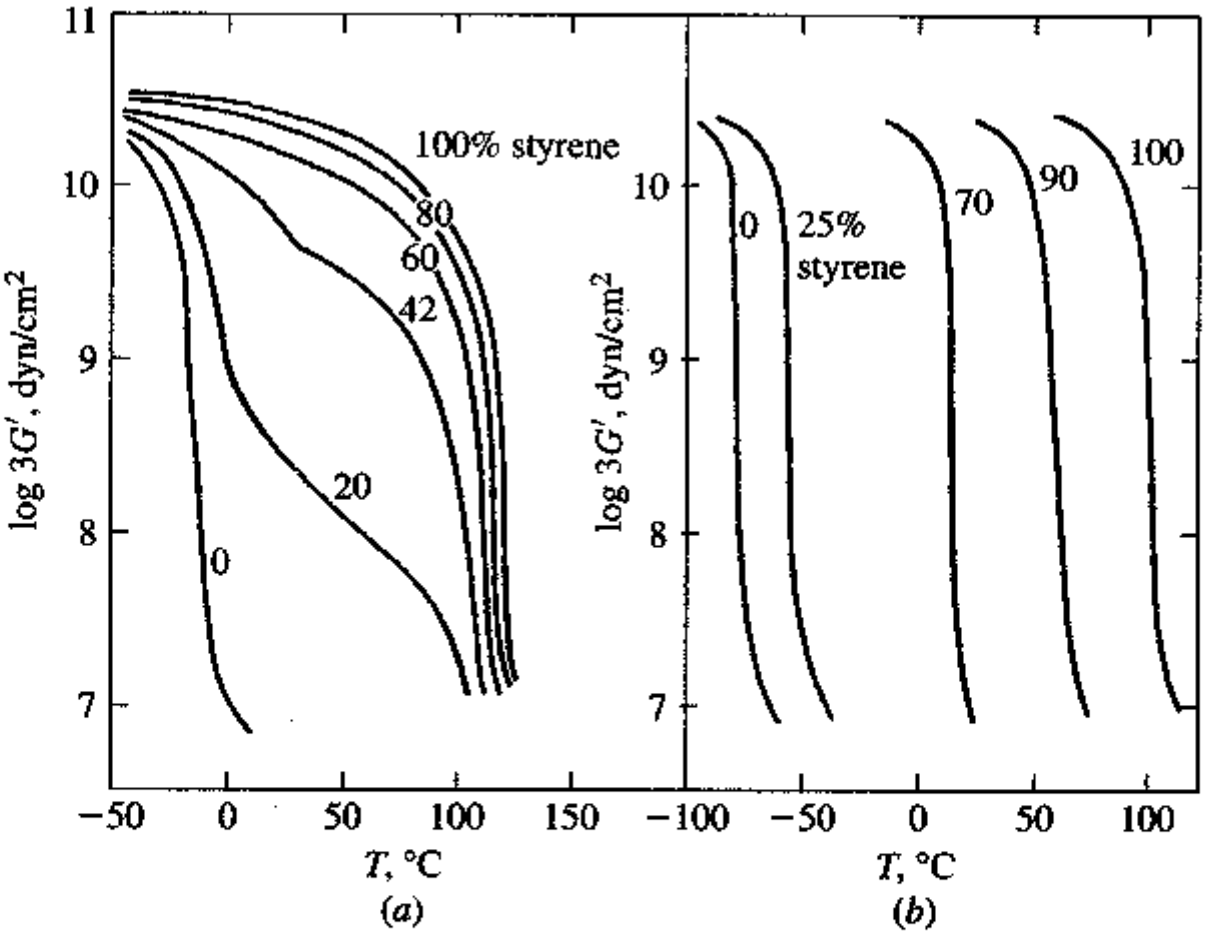

Figure 6.39 Modulus versus temperature for (*a*) styrene isoprene block copolymers and (*b*) styrene butadiene random copolymers as a function of styrene content; from Cooper and Tobolsky [52]. *Source:* From "Properties of linear elastomeric polyurethanes," by S. L. Cooper and A. V. Tobolsky, *Journal of Applied Polymer Science,* Copyright © 1966 by John Wiley & Sons, Inc. Reprinted by permission of John Wiley & Sons, Inc.

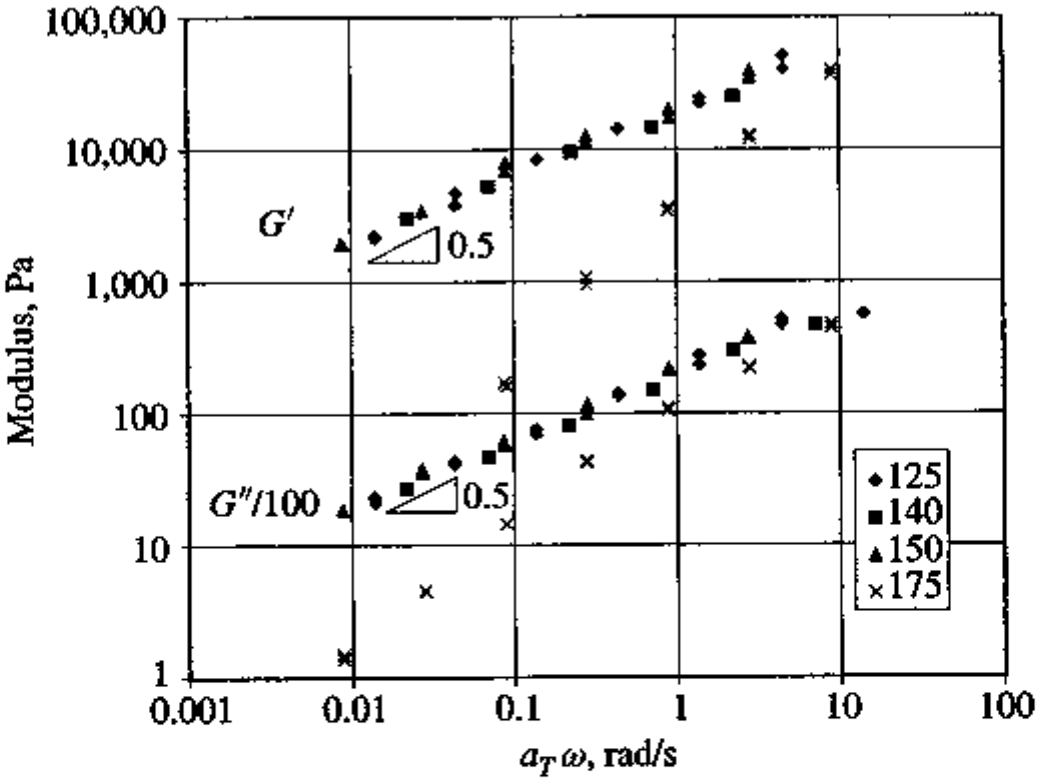

Figure 6.40 Linear viscoelastic moduli $G'(\omega)$ and $G''(\omega)$ for a polystyrene–polybutadiene–polystyrene block copolymer (block M_w =7–43–7 kg/mol) [47]; from Chung and Gale. The data have been time–temperature shifted to a reference temperature of 125°C. The moduli at low frequency do not follow the power laws $G' \propto \omega^2$ and $G'' \propto \omega$ that are exhibited by linear polymers. Rather for microphase-separated block copolymers $G' \propto \omega^{0.5}$ and $G'' \propto \omega^{0.5}$. At 175°C the microphase structure is melted, $G' \propto \omega^{1.2}$ and $G'' \propto \omega^{0.84}$. *Source:* From "Newtonian behavior of a styrene-butadiene-styrene block copolymer," by C. I. Chung and J. C. Gale, *Journal of Polymer Science, Polymer Physics Edition*, Copyright © 1976 by John Wiley & Sons. Reprinted by permission of John Wiley & Sons, Inc.

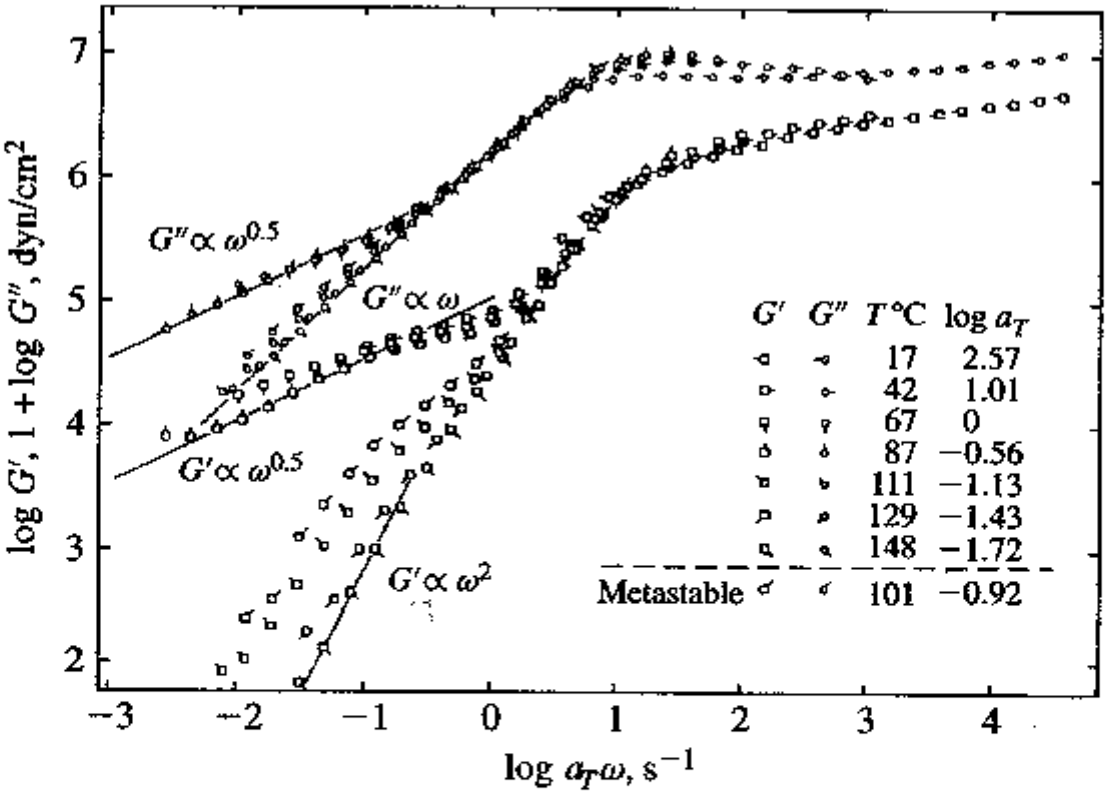

Figure 6.41 Linear viscoelastic moduli $G'(\omega)$ and $G''(\omega)$ for a 1,4-polybutadiene–1,2-polybutadiene block copolymer (block M_w =27.3–44.5 kg/mol) [14]; from Bates. The data have been time–temperature shifted to a reference temperature of 67°C. Near 100°C the microphase structure is melted, and at the highest temperature shown $G' \propto \omega^2$ and $G'' \propto \omega^1$. *Source:* Reprinted with permission, "Block copolymers near the microphase separation transition. 2. Linear dynamic mechanical properties," F. Bates, *Macromolecules*, **17**, 2607–2613 (1984). Copyright © 1984, American Chemical Society.

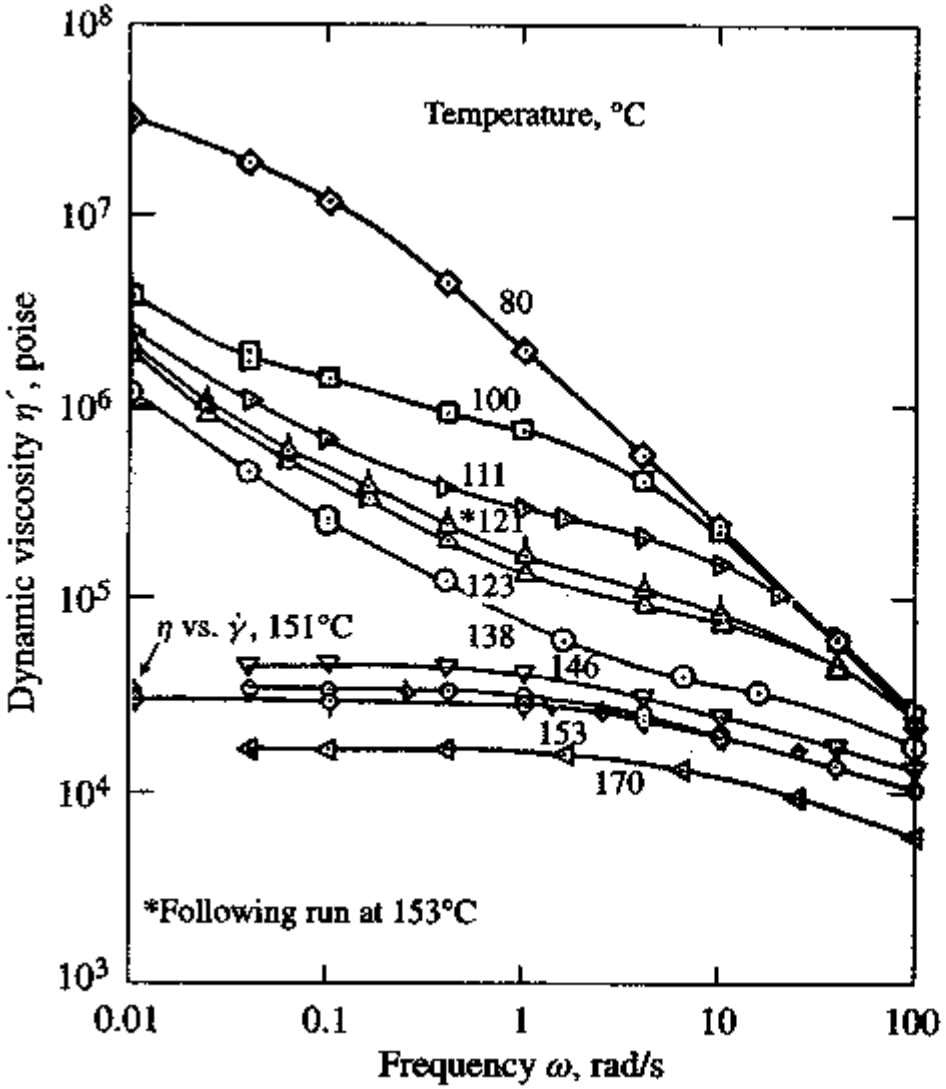

Figure 6.42 Dynamic viscosity η' versus frequency ω and steady shear viscosity η versus shear rate $\dot{\gamma}$ for a (*b*)polystyrene–(*b*)polybutadiene–(*b*)polystyrene triblock copolymer of block M_w = 7(PS)–43(PB)–7(PS) kg/mol; from Gouinlock and Porter [94]. For η' various temperatures are shown as indicated; steady shear viscosity is given at a single temperature, 151°C. At 150°C the block copolymer goes through the microphase-separation transition, and both viscosities become independent of the rate of deformation. *Source:* From *Polymer Engineering and Science,* Copyright © 1977, Society of Plastics Engineers. Reprinted by permission.

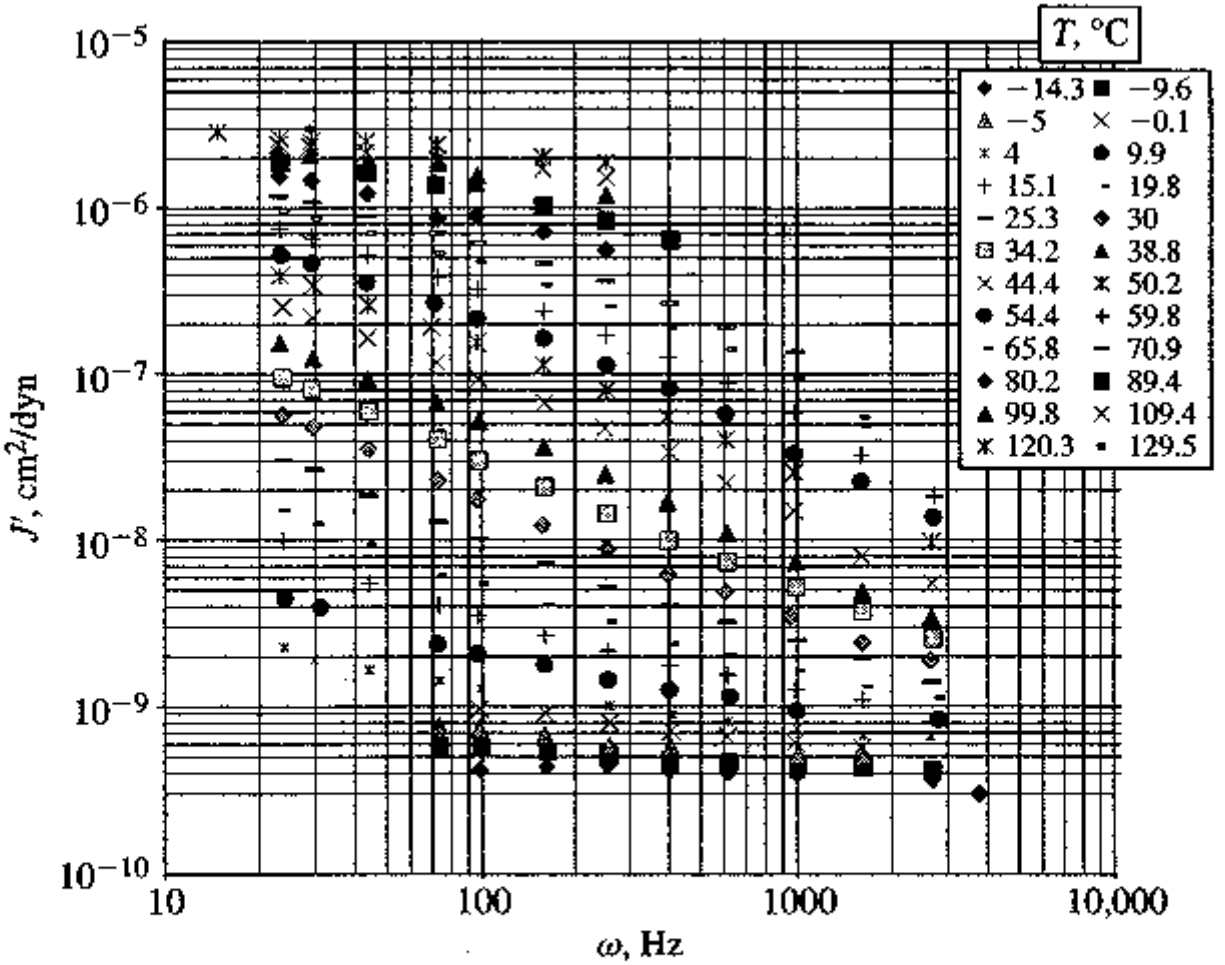

Figure 6.43 Linear viscoelastic storage compliance J' of poly(*n*-octyl methacrylate) as a function of frequency and temperature; replotted from Dannhauser et al. [56]. *Source:* From the *Journal of Colloid Science,* Copyright © 1958, Academic Press. Reprinted by permission.

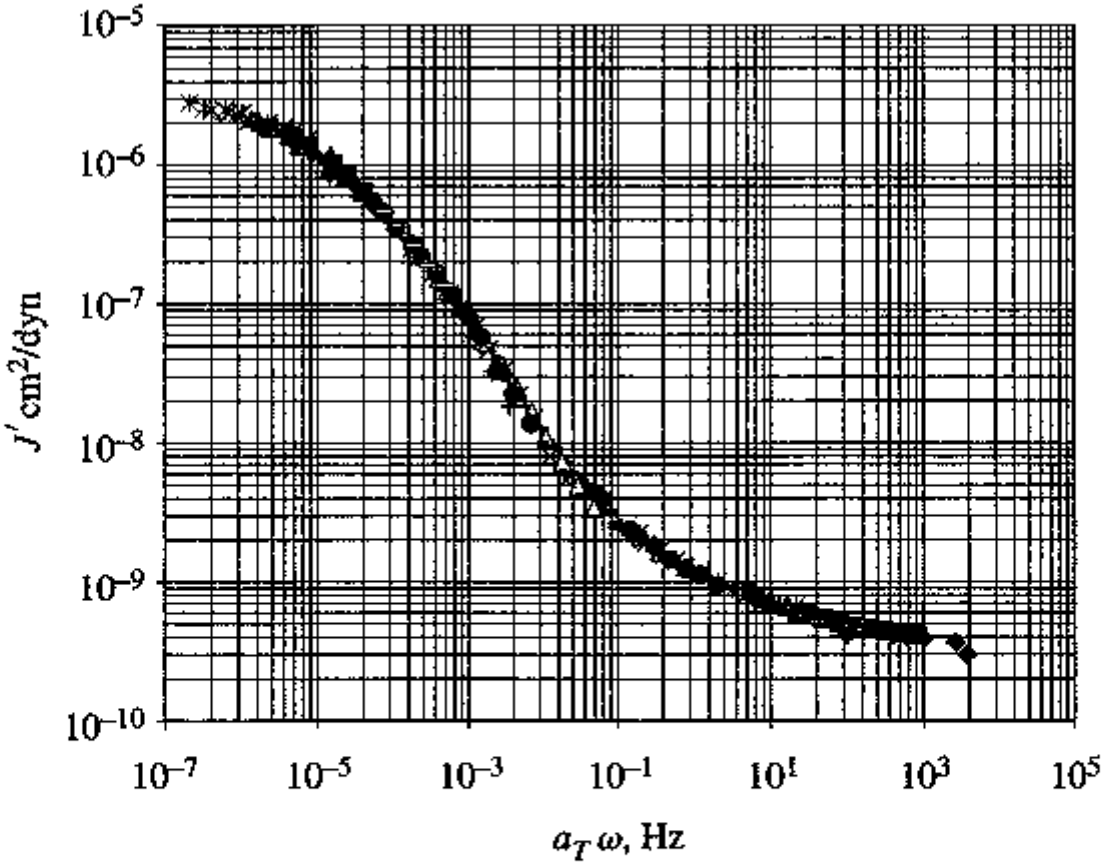

Figure 6.44 Master curve of linear viscoelastic storage compliance J' of poly(*n*-octyl methacrylate) at $T_{ref} = -14.3°C = 258.9$ K as a function of reduced frequency $a_T\omega$; recalculated from data in Figure 6.43 from Dannhauser et al. [56]. *Source:* From the *Journal of Colloid Science,* Copyright © 1958, Academic Press. Reprinted by permission.

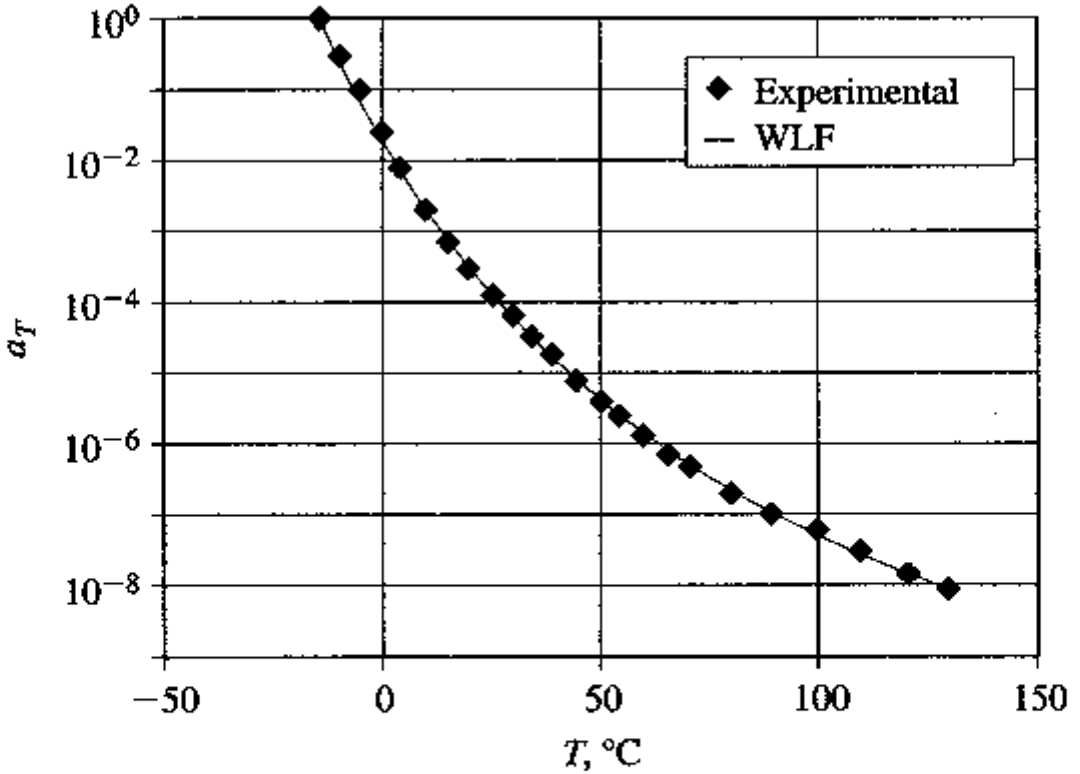

Figure 6.45 Shift parameters versus temperature for poly (*n*-octyl methacrylate) in Figure 6.44; $T_{ref} = -14.3°C = 258.9K$. Also included is the fit to the WLF equation; calculated from data in Dannhauser et al. [56]. *Source:* From the *Journal of Colloid Science*, Copyright © 1958, Academic Press. Reprinted by permission.

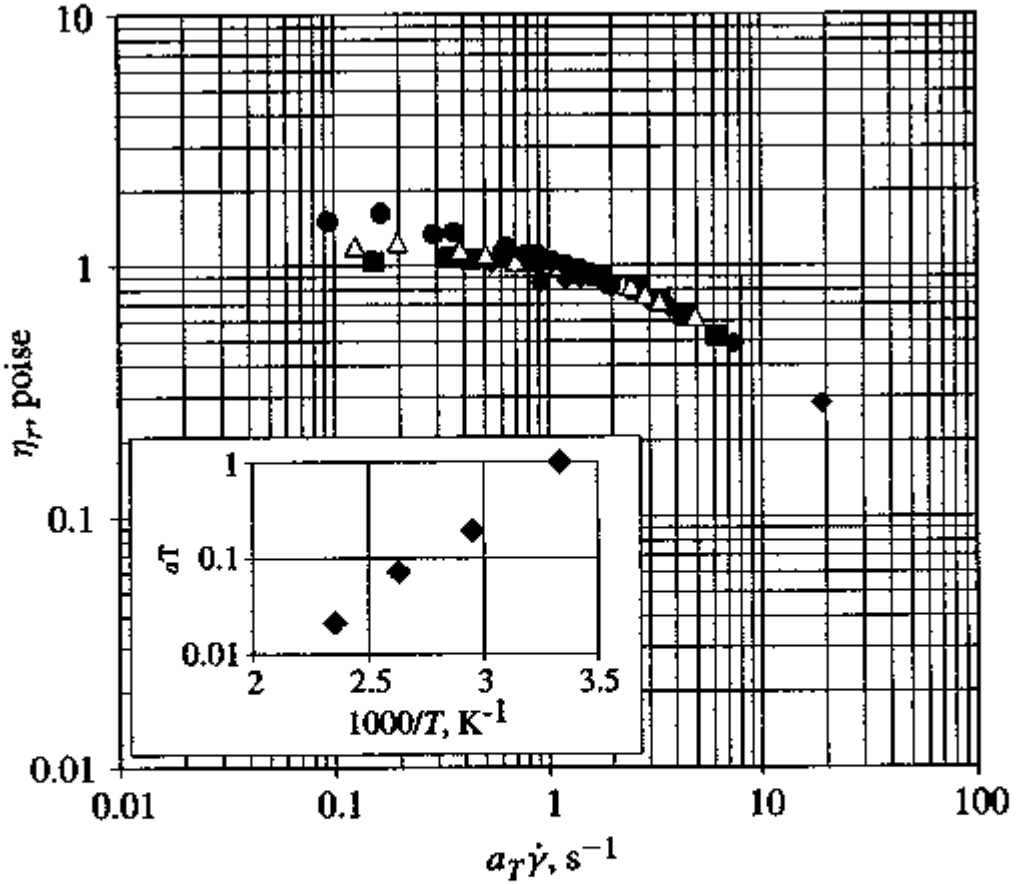

Figure 6.46 Master curve of steady shear viscosity η_r versus reduced shear rate $a_T\dot{\gamma}$ obtained through time–temperature superposition for the polybutadiene data shown in Figure 6.28; $T_{ref} = 300$ K. *Source:* From "Rheological properties of polybutadienes prepared by *n*-butyllithium initiation," by J. T. Gruver and G. Kraus, *Journal of Polymer Science, Part A*, Copyright © 1964 by John Wiley & Sons, Inc. Reprinted by permission of John Wiley & Sons, Inc.

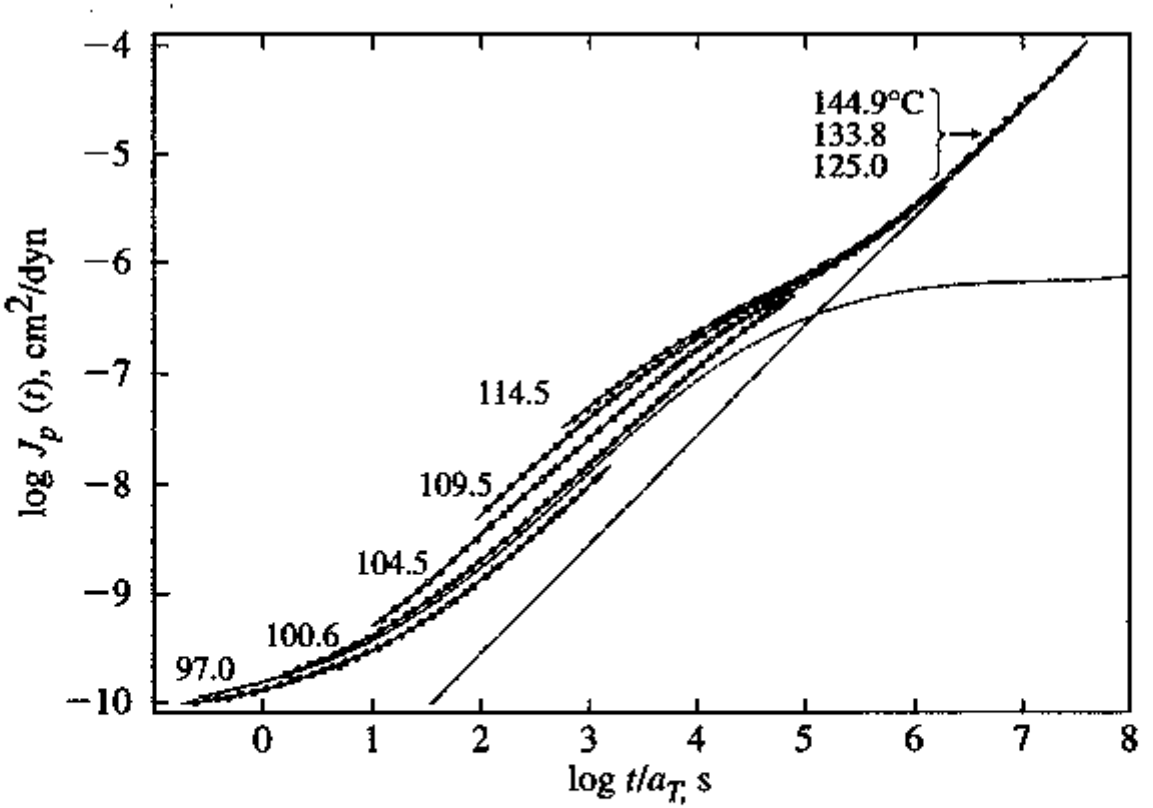

Figure 6.47 Shear creep compliance corrected for vertical shift, $J_p(t) = J(t)T\rho/(T_{\text{ref}}\rho_{\text{ref}})$, versus shifted time, t/a_T for nearly monodisperse polystyrene (46.9 kg/mol) reduced to $T_{\text{ref}} = 100°\text{C}$ by using values of a_T calculated from $a_T = \eta(T)/\eta(T_{\text{ref}})$; from Plazek [209]. Poor superposition is seen due to the proximity of T_g for the lower experimental temperatures. *Source:* Reprinted with permission from "Temperature dependence of the viscoelastic behavior of polystyrene," D. J. Plazek, *Journal of Physical Chemistry*, **69**, 3480–3487 (1965). Copyright © 1965, American Chemical Society.

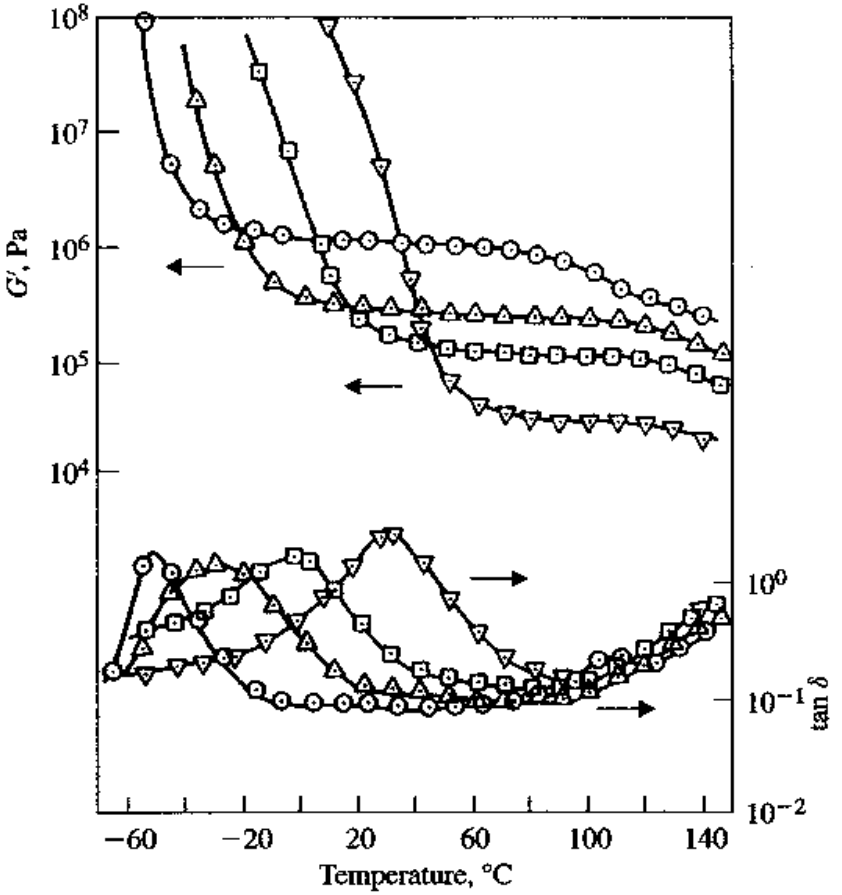

Figure 6.48 Storage modulus G' and $\tan\delta$ for a block copolymer (Kraton 1111, (*b*)polystyrene–(*b*)polyisoprene–(*b*)polystyrene block copolymer, Shell Development Company) and three mixtures with tackifier (Piccotac 95BHT, a hydrocarbon resin; Hercules, Inc.) showing that adding the tackifier reduces the plateau modulus and moves the glass transition to higher temperatures (transition zone shifts to the right): ○, Kraton 1111; △, 30 wt % tackifier; □, 50 wt % tackifier; ▽, 70 wt % tackifier; from Kim et al. [126]. *Source:* From "Viscoelastic behavior and order-disorder transition in mixtures of a block copolymer and a midblock-associating resin," by J. Kim, C. D. Han, and S. G. Chu, *Journal of Polymer Science, Polymer Physics Edition*, Copyright © 1988 by John Wiley & Sons, Inc. Reprinted by permission of John Wiley & Sons, Inc.

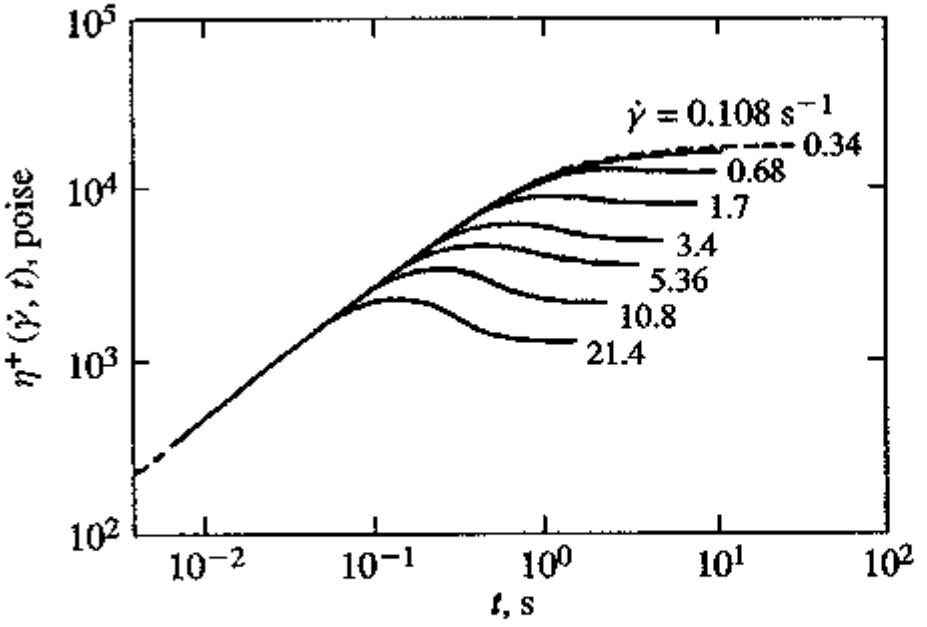

Figure 6.49 Shear-stress growth function as a function of time t at several shear rates for a concentrated solution of a narrowly distributed polybutadiene; from Menezes and Graessley [177]. $M_w = 350$ kg/mol; $M_w/M_n < 1.05$; concentration = 0.0676 g/cm^3 in Flexon 391, a hydrocarbon oil. *Source:* From "Nonlinear rheological behavior of polymer systems for several shear-flow histories," by E. V. Menezes and W. W. Graessley, *Journal of Polymer Science, Polymer Physics Edition*,

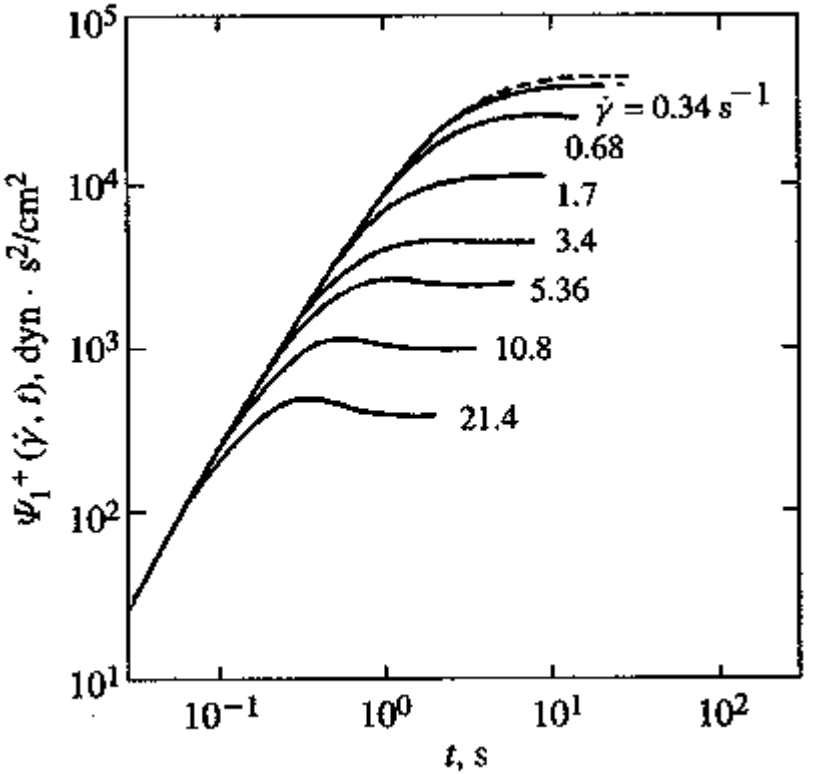

Figure 6.50 First normal-stress growth function as a function of time t at several shear rates for a concentrated solution of a narrowly distributed polybutadiene; from Menezes and Graessley [177]. M_w = 350 kg/mol, $M_w/M_n < 1.05$; concentration = 0.0676 g/cm^3 in Flexon 391, a hydrocarbon oil. *Source:* From "Nonlinear rheological behavior of polymer systems for several shear-flow histories," by E. V. Menezes and W. W. Graessley, *Journal of Polymer Science, Polymer Physics Edition*, Copyright © 1982 by John Wiley & Sons, Inc. Reprinted by permission of John Wiley & Sons, Inc.

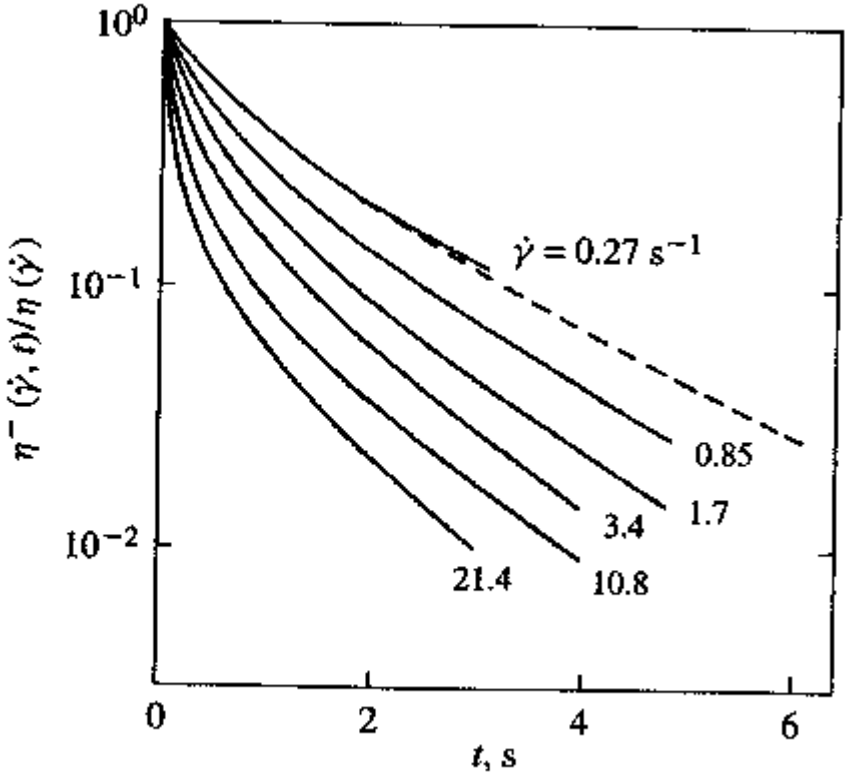

Figure 6.51 Normalized shear stress cessation function versus time since cessation of flow t at several shear rates $\dot{\gamma}$ for a concentrated solution of a narrowly distributed polybutadiene; from Menezes and Graessley [177]. $M_w = 350$ kg/mol; $M_w/M_n < 1.05$; concentration $= 0.0676$ g/cm^3 in Flexon 391, a hydrocarbon oil. *Source:* From "Nonlinear rheological behavior of polymer systems for several shear-flow histories," by E. V. Menezes and W. W. Graessley, *Journal of Polymer Science, Polymer Physics Edition*, Copyright © 1982 by John Wiley & Sons, Inc. Reprinted by permission of John Wiley & Sons, Inc.

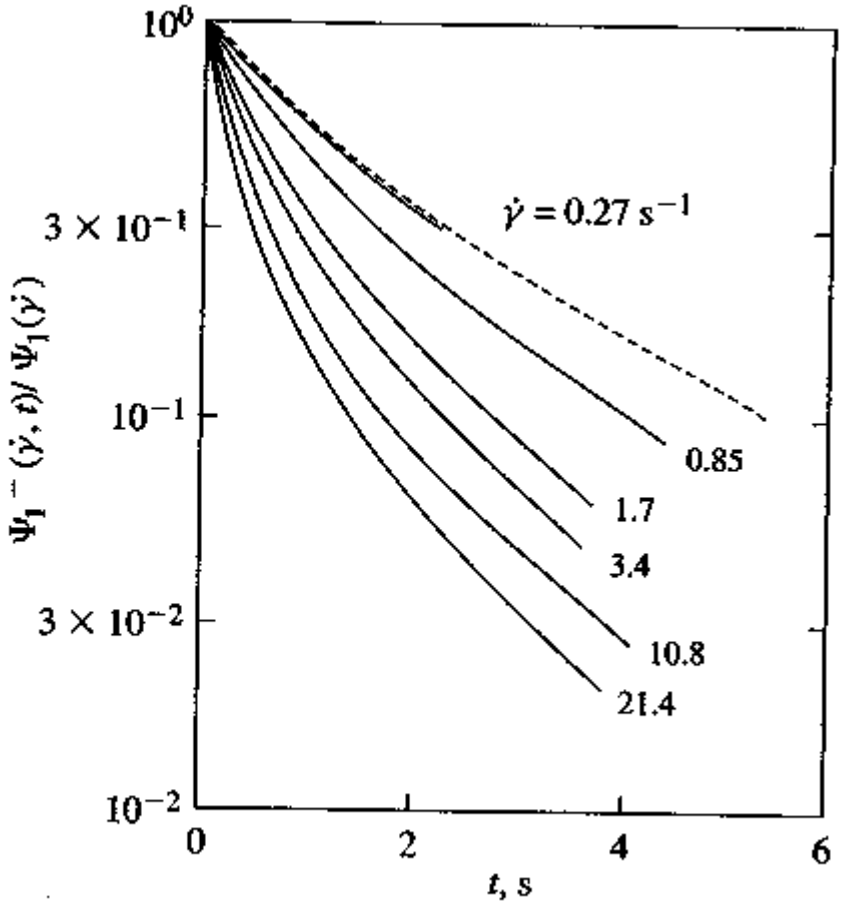

Figure 6.52 First normal-stress stress cessation function at several shear rates for a concentrated solution of a narrowly distributed polybutadiene; from Menezes and Graessley [177]. $M_w = 350$ kg/mol; $M_w/M_n < 1.05$; concentration = 0.0676 g/cm^3 in Flexon 391, a hydrocarbon oil. *Source:* From "Nonlinear rheological behavior of polymer systems for several shear-flow histories," by E. V. Menezes and W. W. Graessley, *Journal of Polymer Science, Polymer Physics Edition*, Copyright © 1982 by John Wiley & Sons, Inc. Reprinted by permission of John Wiley & Sons, Inc.

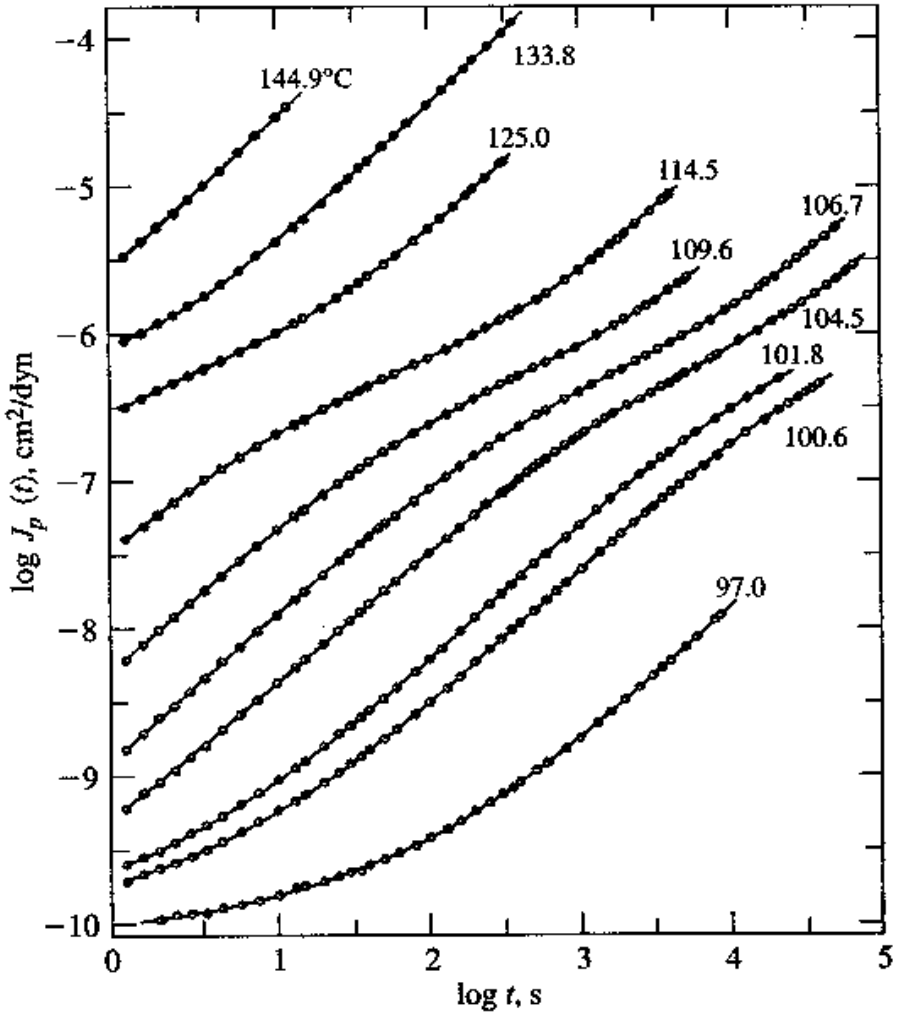

Figure 6.53 Shear creep compliance corrected for vertical shift, $J_p(t) = J(t)T\rho/(T_{\text{ref}}\rho_{\text{ref}})$, of nearly monodisperse polystyrene (46.9 kg/mol) at various temperatures; from Plazek [209]. *Source:* Reprinted with permission from "Temperature dependence of the viscoelastic behavior of polystyrene," D. J. Plazek, *Journal of Physical Chemistry*, **69**, 3480–3487 (1965). Copyright © 1965, American Chemical Society.

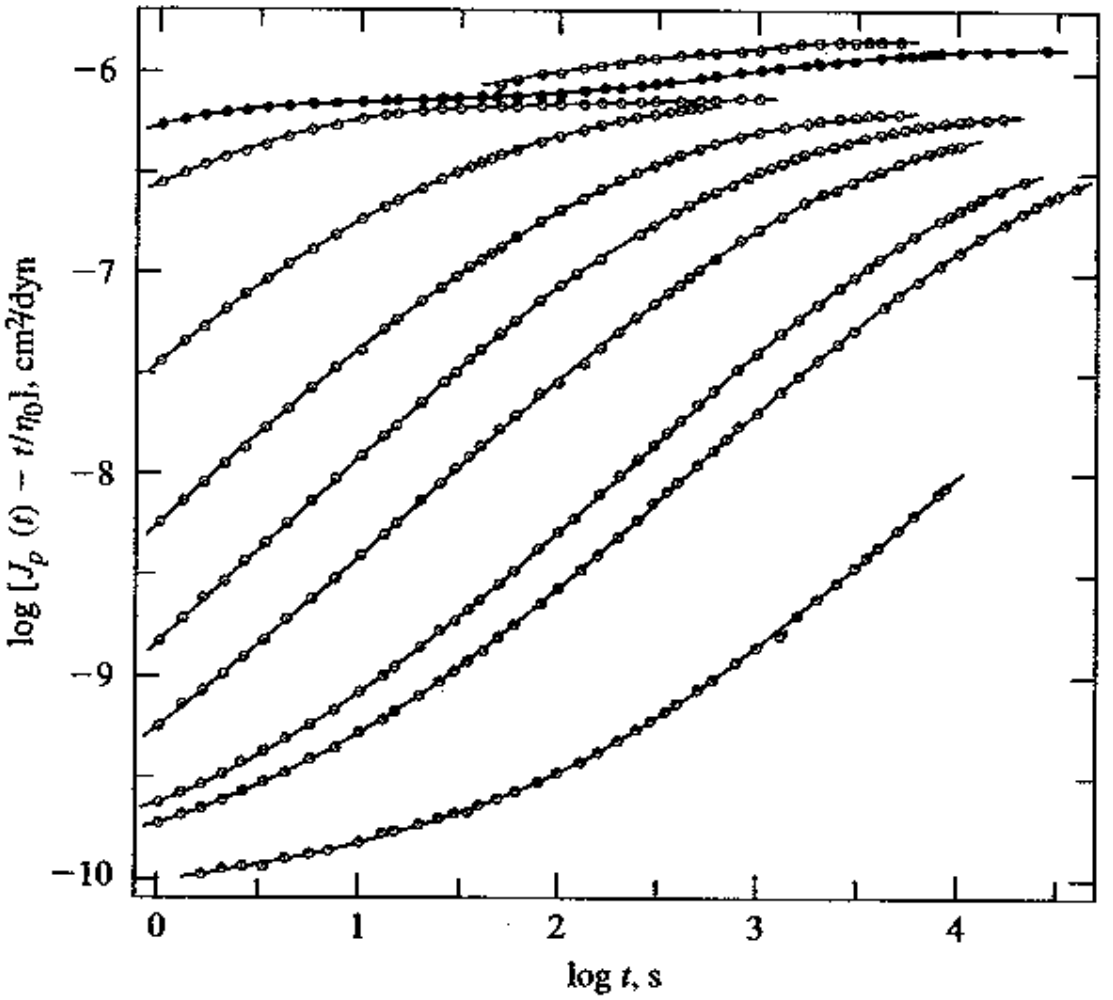

Figure 6.54 Recoverable shear creep compliance $J_p - t/\eta_0$ of nearly monodisperse polystyrene (46.9 kg/mol). Data have been corrected for vertical shift, $J_p(t) = J(t)T\rho/(T_{\text{ref}}\rho_{\text{ref}})$; from Plazek [209]. *Source:* Reprinted with permission from "Temperature dependence of the viscoelastic behavior of polystyrene," D. J. Plazek, *Journal of Physical Chemistry*, **69**, 3480–3487 (1965). Copyright © 1965, American Chemical Society.

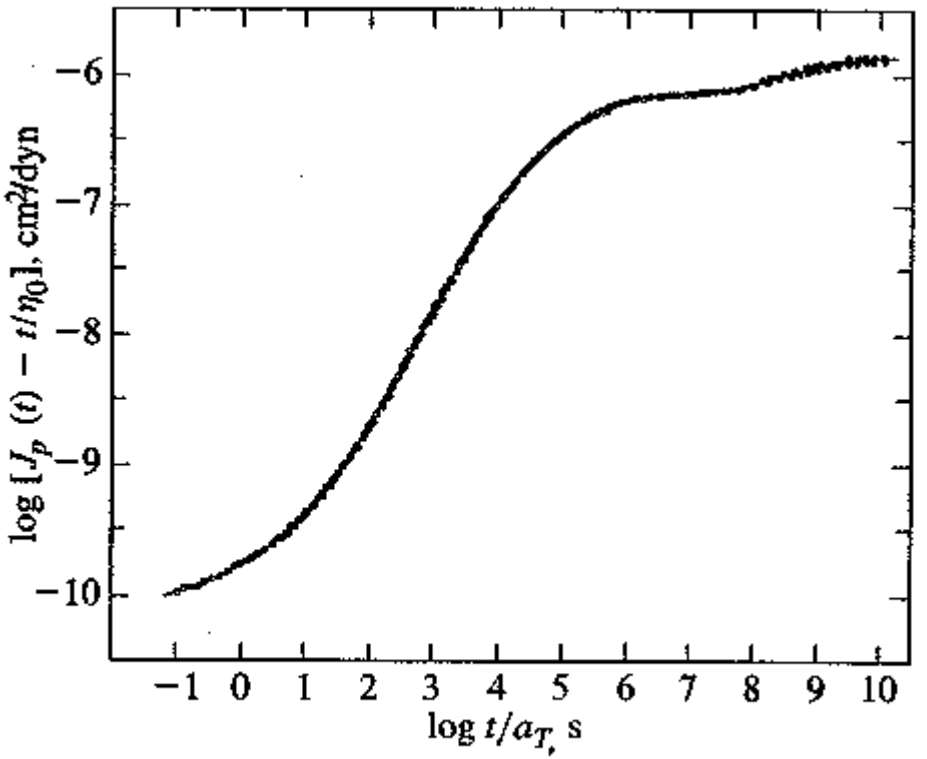

Figure 6.55 Master curve at 100°C of recoverable shear compliance versus time t of a nearly monodisperse polystyrene (46.9 kg/mol) calculated from the data in Figure 6.54; from Plazek [209]. *Source:* Reprinted with permission from "Temperature dependence of the viscoelastic behavior of polystyrene," D. J. Plazek, *Journal of Physical Chemistry*, **69**, 3480–3487 (1965). Copyright © 1965, American Chemical Society.

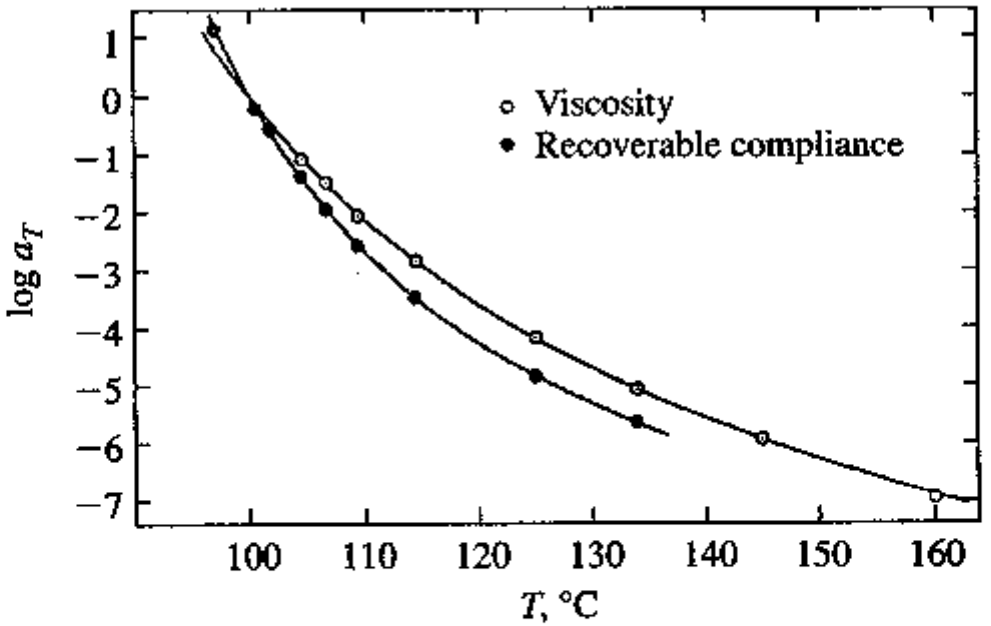

Figure 6.56 Shift factors as a function of temperature. ○, values calculated from viscosity [Equation (6.14)], ●, values used to produce the master curve of recoverable compliance in Figure 6.55 for monodisperse polystyrene (46.9 kg/mol; $T_{ref} = 100°C$); from Plazek [209]. *Source:* Reprinted with permission from "Temperature dependence of the viscoelastic behavior of polystyrene," D. J. Plazek, *Journal of Physical Chemistry*, **69**, 3480–3487 (1965). Copyright © 1965, American Chemical Society.

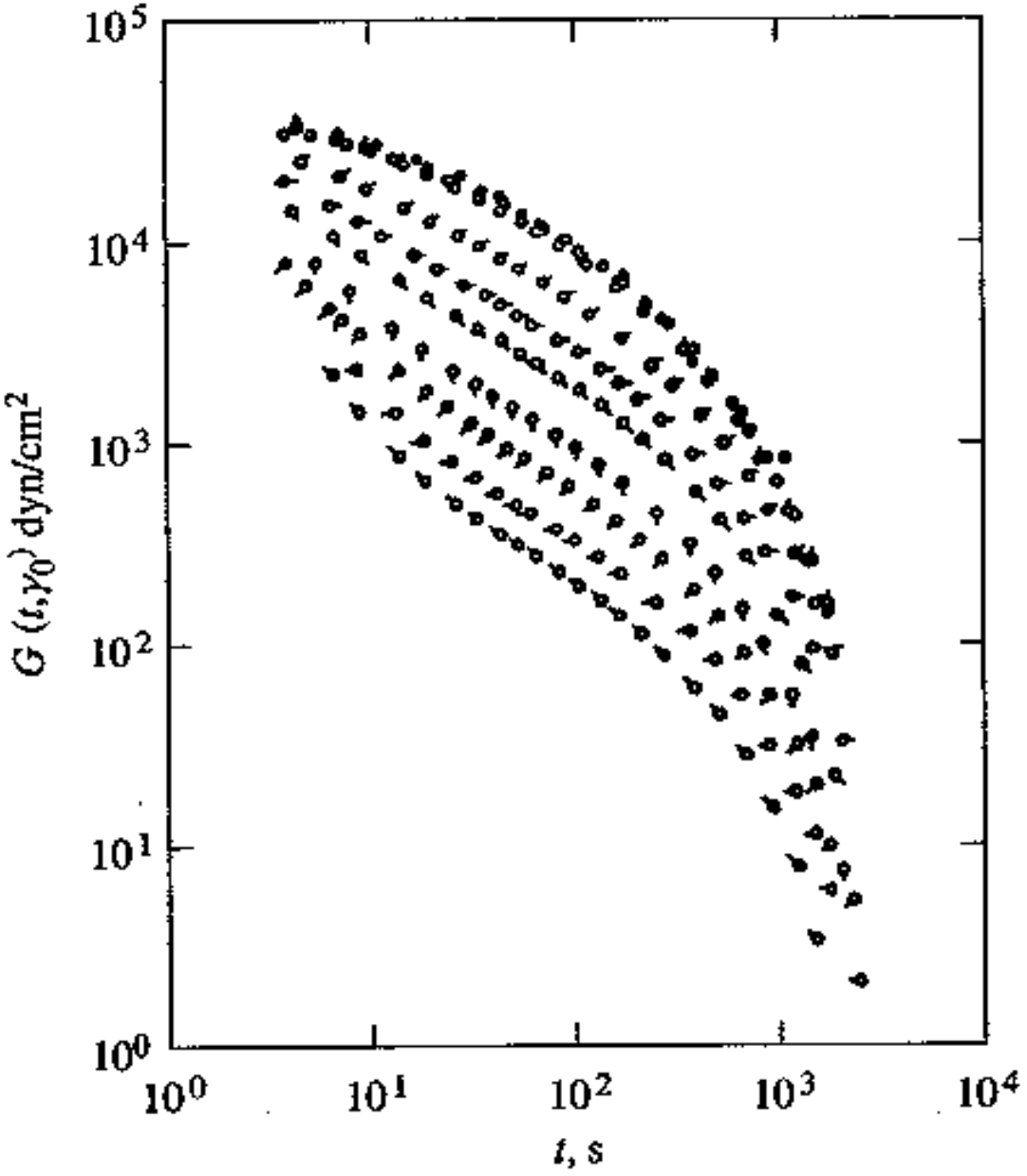

Figure 6.57 Nonlinear shear relaxation modulus $G(t, \gamma_0)$ as a function of time t at 33.5°C, measured in relaxation after step shear strain for 20% solutions of narrow molecular-weight-distribution polystyrene ($M_w = 1.8 \times 10^6$) in chlorinated diphenyl; from Einaga et al. [72]. Different curves are for different strain amplitudes γ_0: ○, $\gamma_0 = 0.41$; pip up $\gamma_0 = 1.87$; for successive clockwise 45° rotations of pip, $\gamma_0 = 3.34$, 5.22, 6.68, 10.0, 13.4, 18.7, and 25.4. *Source:* From *Polymer Journal*, Copyright © 1971, The Society of Polymer Science, Japan. Reprinted by permission.

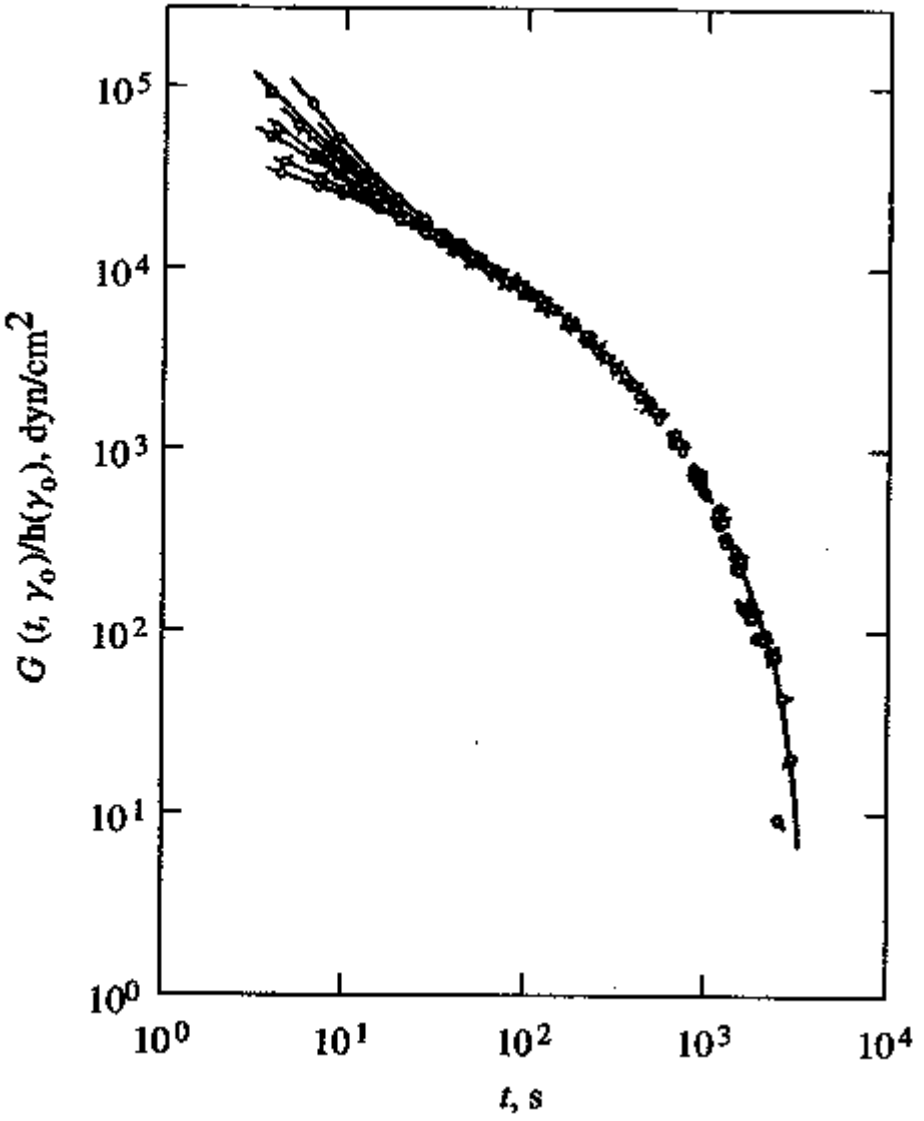

Figure 6.58 Shifted relaxation modulus $G(t, \gamma_0)/h(\gamma_0)$ at 33.5°C for the polystyrene solution data shown in Figure 6.57; from Einaga et al. [72]. $h(\gamma_0)$ is the damping function and is equal to $G(t, \gamma_0)/G(t)$, where $G(t)$ is the relaxation modulus at small strains, and $\log h$ is the vertical shift required to superpose the curves of Figure 6.57. Symbols are the same as in Figure 6.57. *Source:* From *Polymer Journal*, Copyright © 1971, The Society of Polymer Science, Japan. Reprinted by permission.

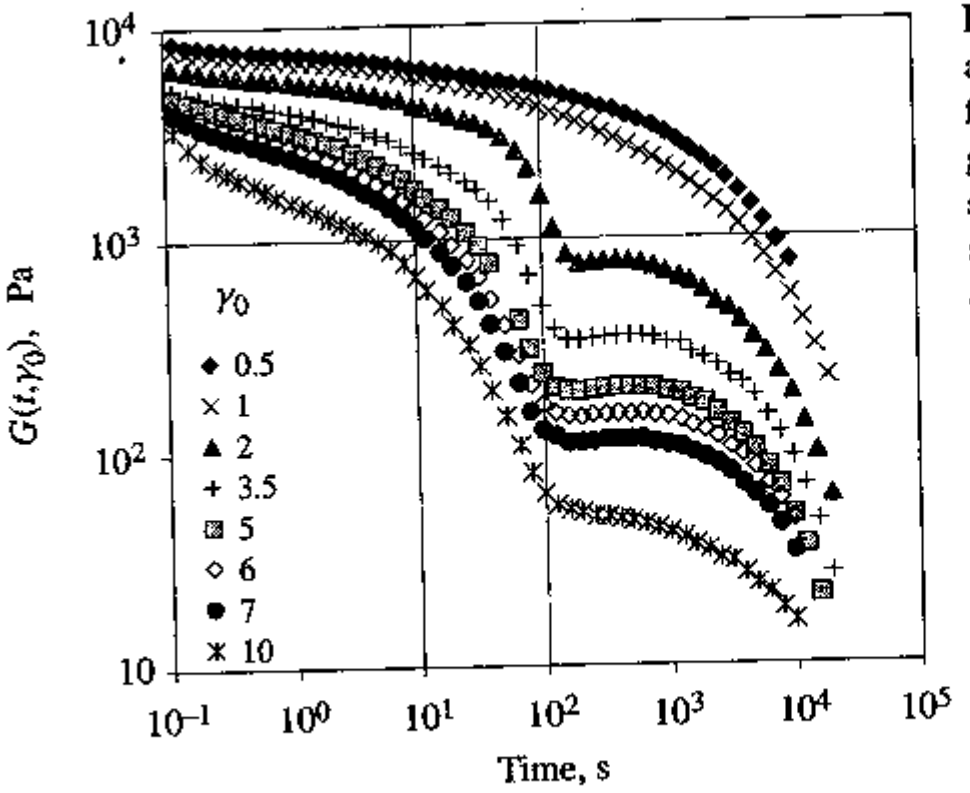

Figure 6.59 Nonlinear shear relaxation modulus $G(t, \gamma_0)$ versus time for a concentrated solution ($c = 0.23$ g/cm^3) of nearly monodisperse polystyrene (8.42×10^6 g/mol) in tricresyl phosphate; 30°C; from Morrison and Larson [184].

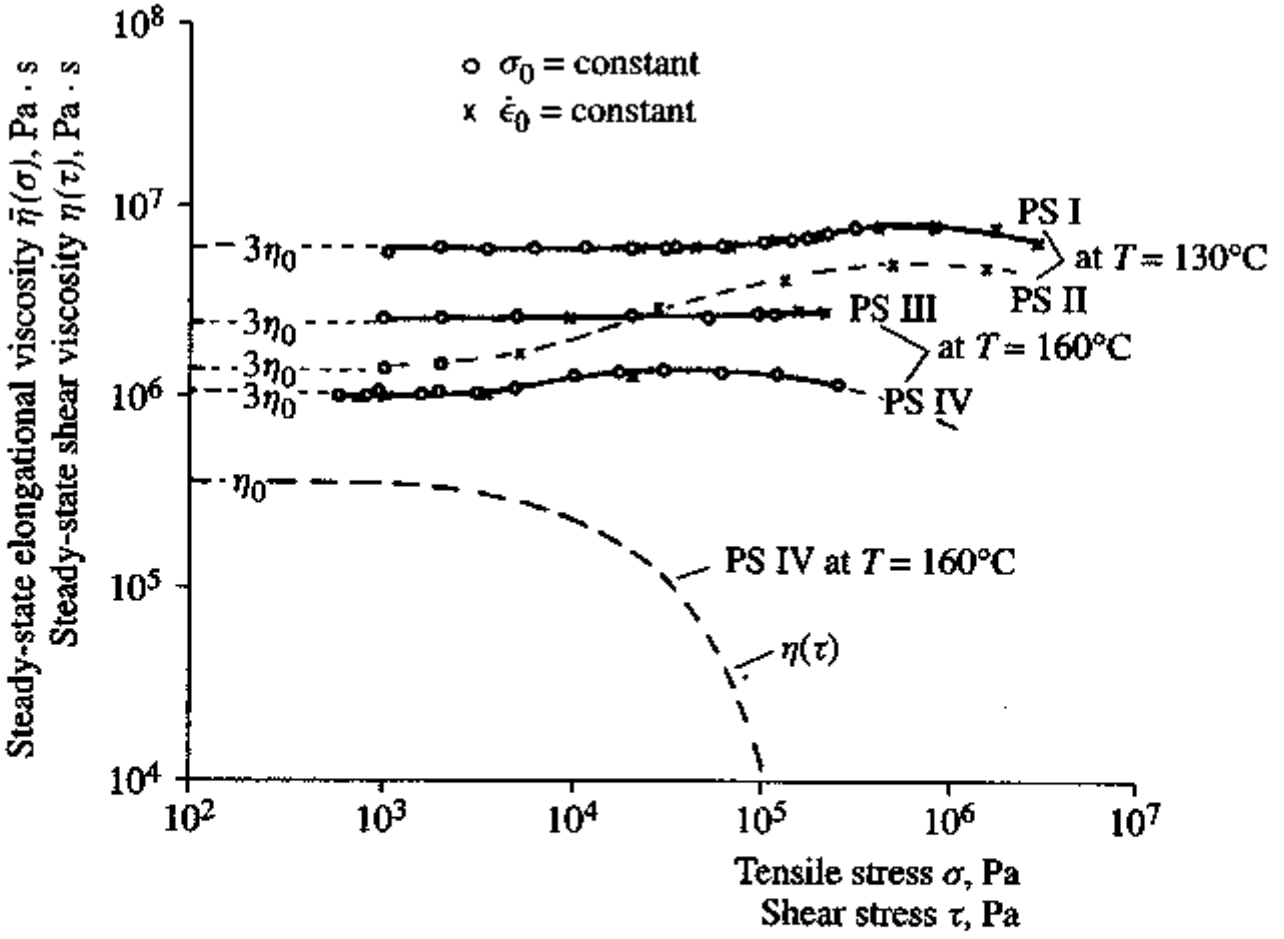

Figure 6.60 Steady uniaxial elongational viscosities $\bar{\eta}(\sigma)$ of several polystyrenes at the temperatures indicated; from Münstedt [187]. The elongational viscosities are plotted as a function of $\sigma = \tau_{33} - \tau_{11}$, while shear viscosity $\eta(\tau)$ for PS IV is plotted as a function of $\tau = \tau_{21}$ Molecular weights: PS I, $M_w = 74$ kg/mol, $M_w/M_n = 1.2$; PS II, $M_w = 39$ kg/mol, $M_w/M_n = 1.1$; PS III, $M_w = 253$ kg/mol, $M_w/M_n = 1.9$; PS IV, $M_w = 219$ kg/mol, $M_w/M_n = 2.3$. *Source:* From the *Journal of Rheology,* Copyright © 1980, The Society of Rheology. Reprinted by permission.

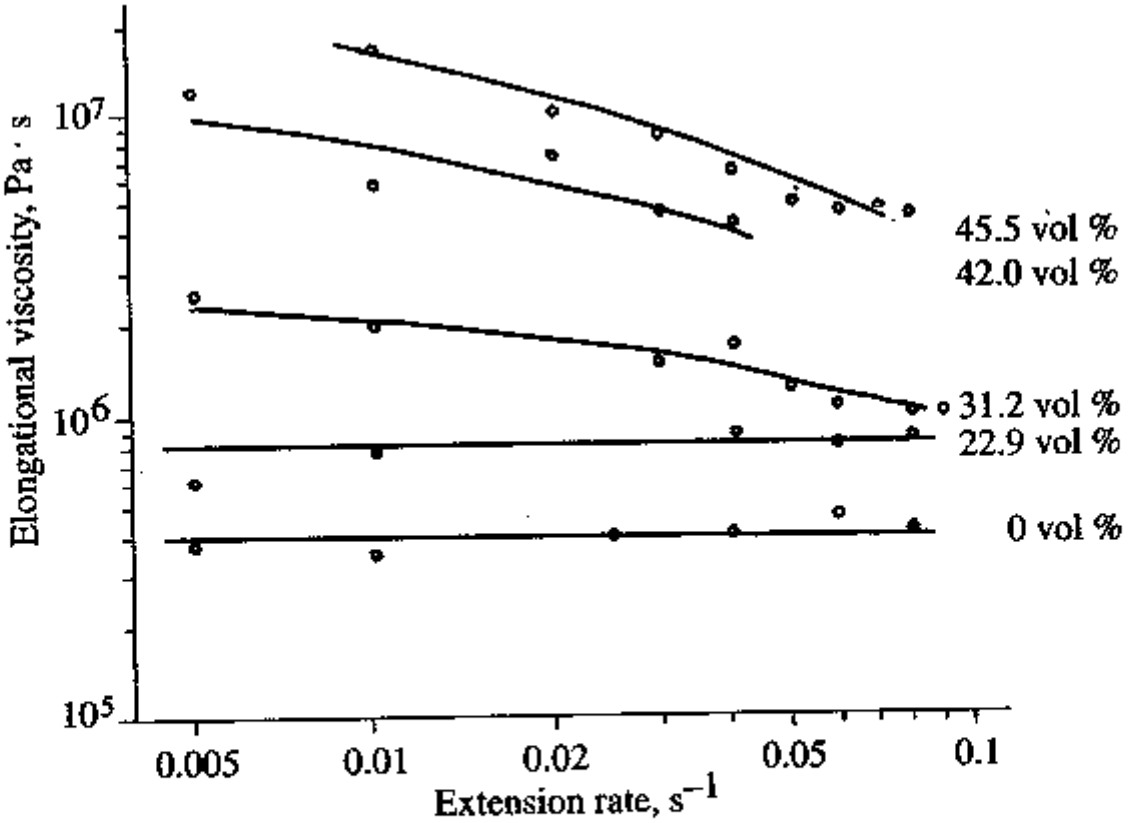

Figure 6.61 Uniaxial elongational viscosity as a function of elongation rate for polyisobutylene (PIB) and PIB filled with α-alumina powder to various volume fractions; from Greener and Evans [101]. The data are at 294 K. The filler causes the PIB to become tension-thinning. *Source:* From the *Journal of Rheology,* Copyright © 1998, The Society of Rheology. Reprinted by permission.

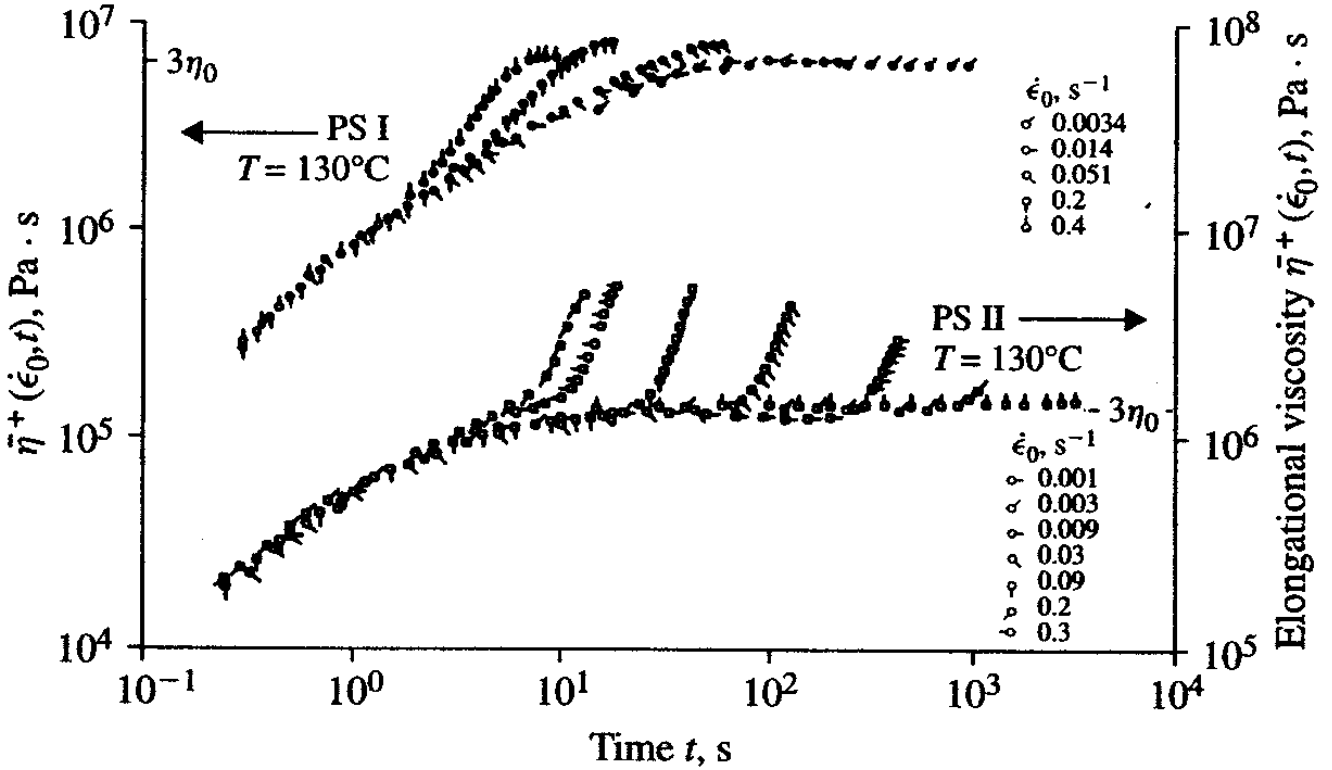

Figure 6.62 Start-up uniaxial elongational viscosity $\bar{\eta}^+(t, \dot{\epsilon}_0)$ versus time t for two polystyrenes at 130°C; from Münstedt [187]. For PS I, $M_w = 74$ kg/mol, $M_w/M_n = 1.2$; for PS II, $M_w = 39$ kg/mol, $M_w/M_n = 1.1$. *Source:* From the *Journal of Rheology,* Copyright © 1980, The Society of Rheology. Reprinted by permission.

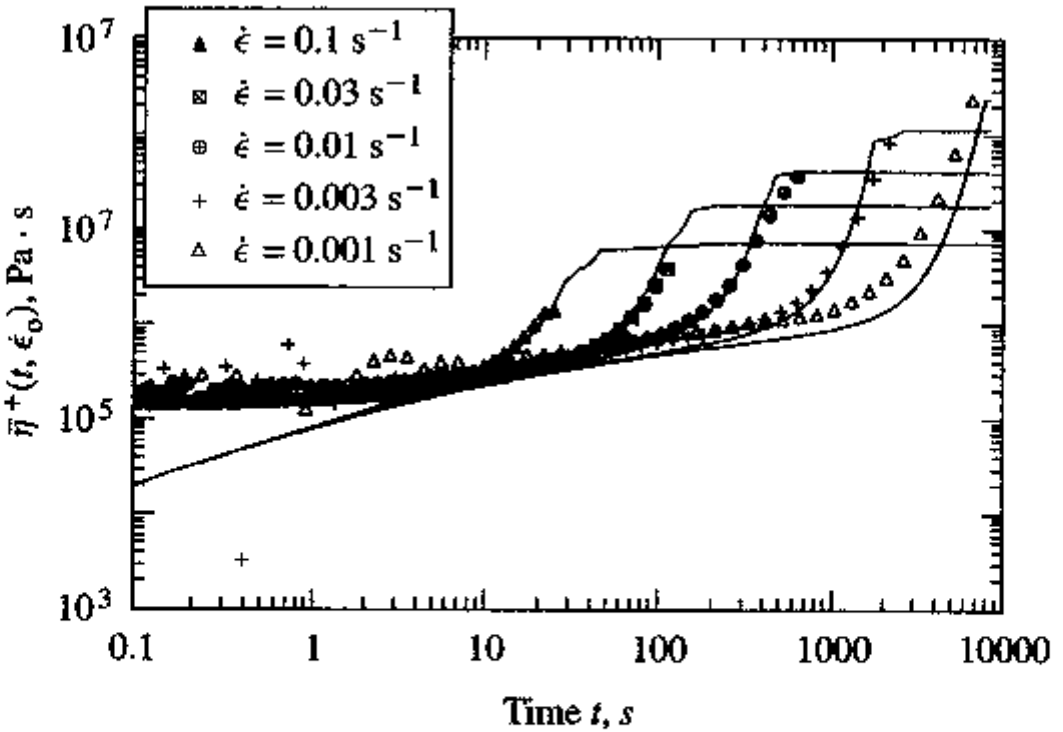

Figure 6.63 Start-up uniaxial elongational viscosity, $\bar{\eta}^+(t, \dot{\epsilon}_0)$ versus time t for low-density polyethylene at 140°C, $M_w = 250$ kg/mol, $M_w/M_n = 15$; from Inkson et al. [130a]. Solid curves represent a fit to a molecular constitutive equation called the 12 mode pompom melt. *Source:* From the *Journal of Rheology*, Copyright © 1999, The Society of Rheology. Reprinted by permission.

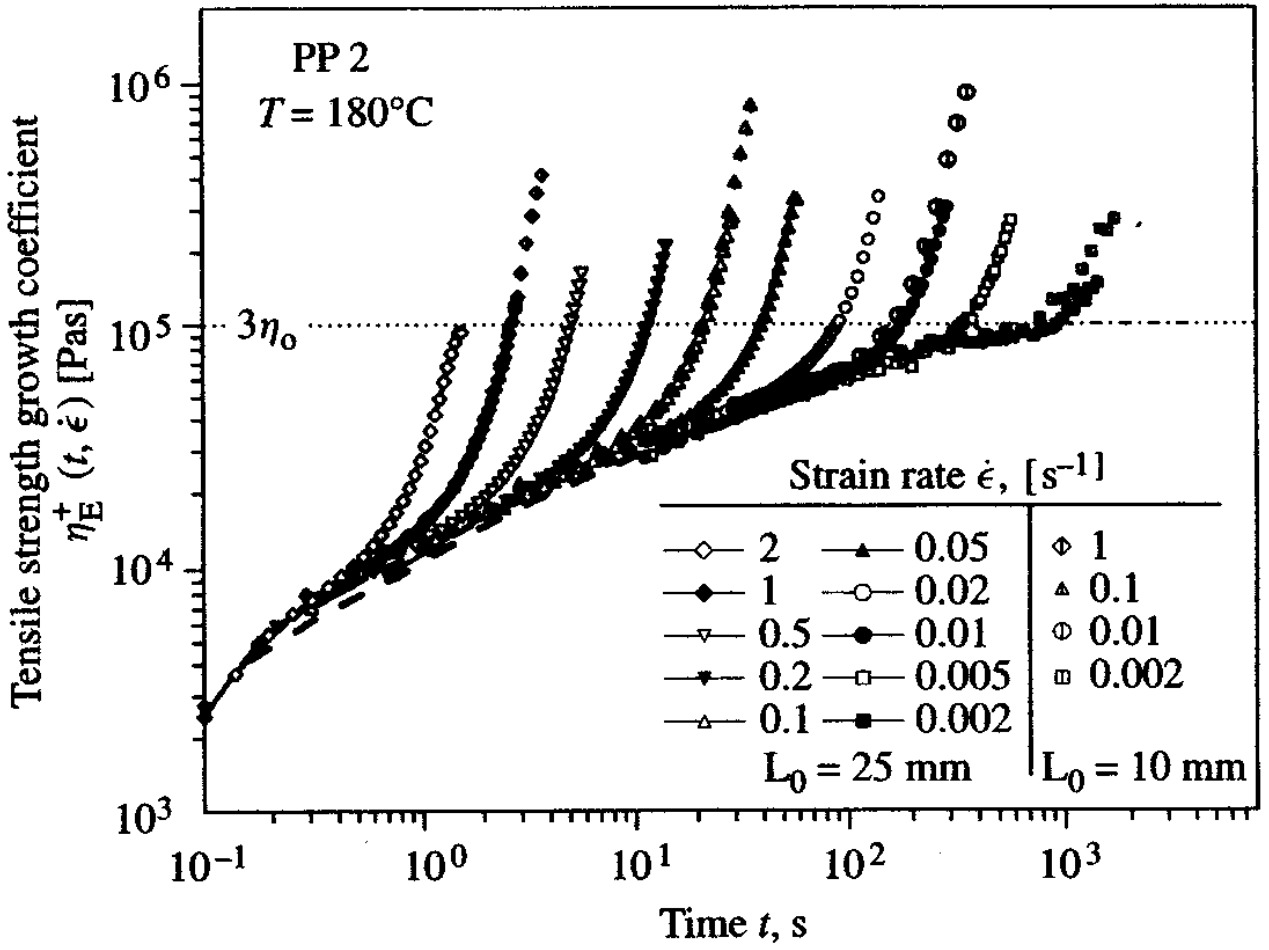

Figure 6.64 Start-up uniaxial elongational viscosity, $\bar{\eta}^+(t, \dot{\epsilon}_0)$, versus time t for polypropylene at 180°C; from Kurzbeck et al. [135]. Two initial sample lengths were used, $L_0 = 25$ mm and 10 mm as indicated on the figure. *Source:* From the *Journal of Rheology,* Copyright © 1999, The Society of Rheology. Reprinted by permission.

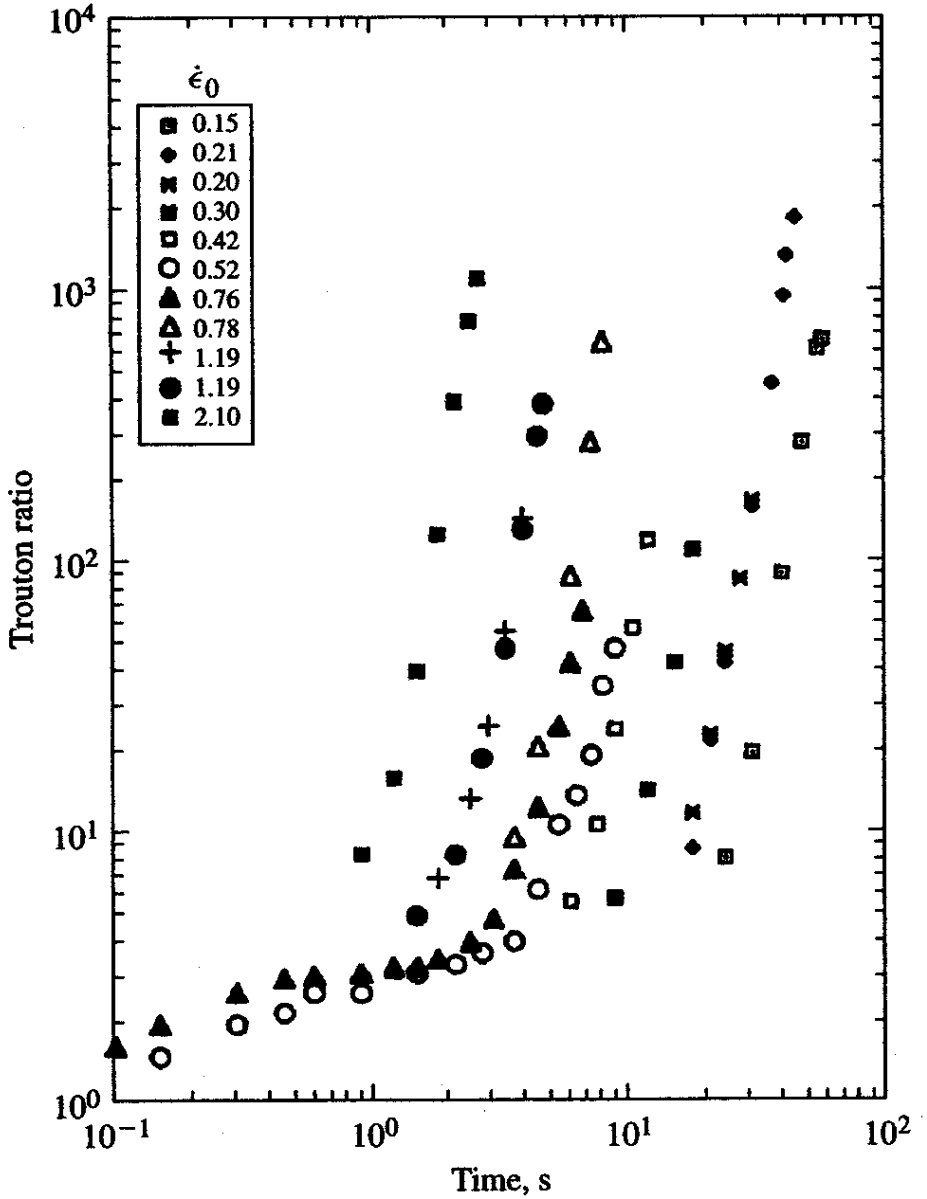

Figure 6.65 Trouton ratio $\mathrm{Tr} = \bar{\eta}^+(t, \dot{\epsilon}_0)/\eta_0$ versus time for a Boger fluid made from 0.185% polyisobutylene in a mixture of kerosene and polybutene; from Sridhar et al. [234]. Since Boger fluids exhibit constant viscosity, Tr versus t has the same shape as the curves of $\bar{\eta}^+$ versus t. *Source:* Reprinted from *Journal of Non-Newtonian Fluid Mechanics*, **40**, T. Sridhar, V. Tirtaatmadja, D. A. Nguyen, and R. K. Gupta, "Measurement of extensional viscosity of polymer solutions," 271–280, Copyright © 1991, with permission from Elsevier Science.

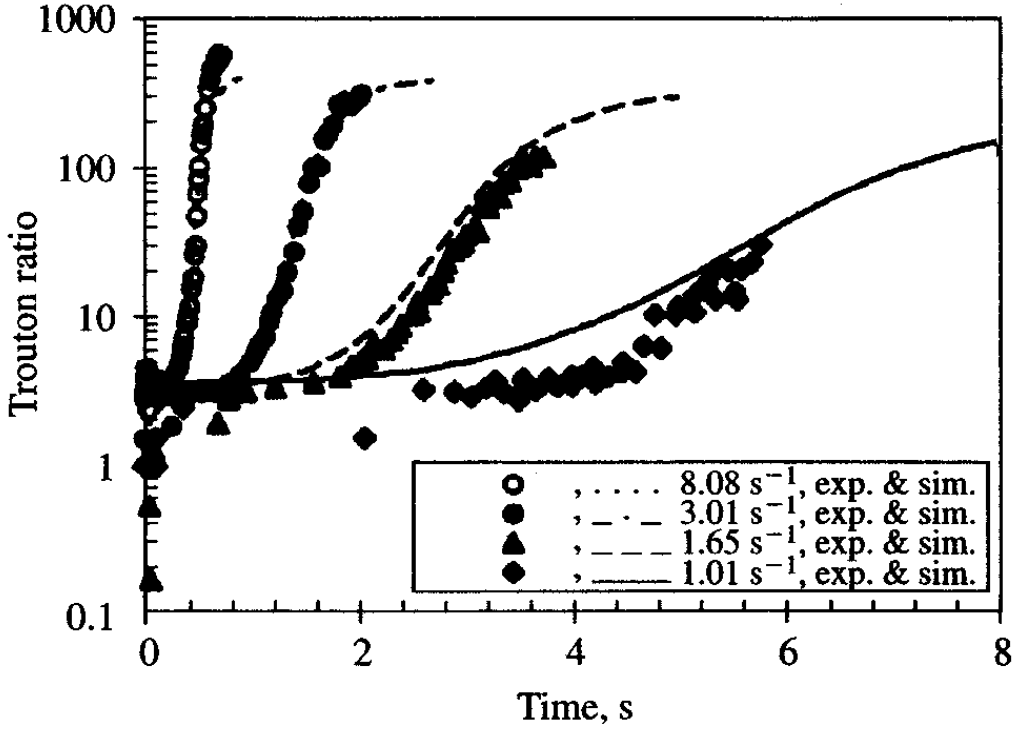

Figure 6.66 Trouton ratio as a function of time for a solution of 1.95×10^6 molecular-weight polystyrene; from Li et al. [153]. The polymer had a narrow molecular weight distribution, and the data were taken at room temperature. The solid and dashed lines are Brownian dynamics simulations of a bead-spring model of polymer solutions. *Source:* From the *Journal of Rheology,* Copyright © 2000, The Society of Rheology. Reprinted by permission.

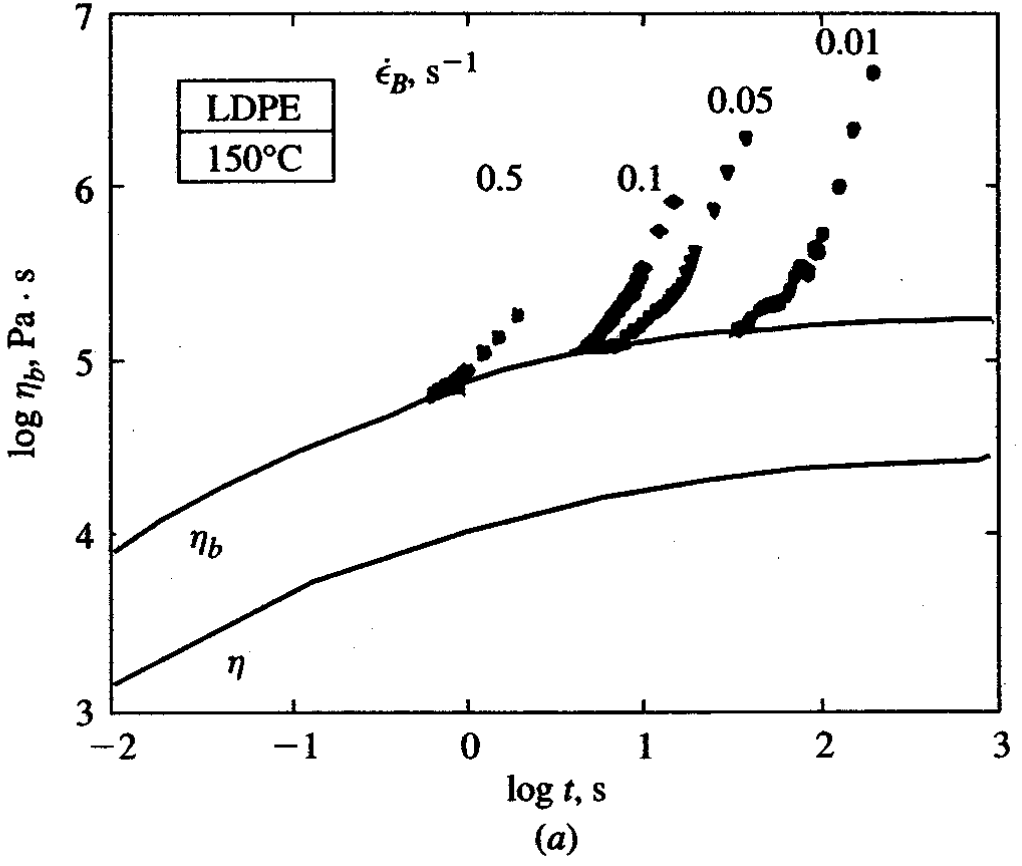

(*a*)

Figure 6.67 Startup of steady biaxial elongation, from Soskey and Winter [230]. (*a*) Low-density polyethylene at 150°C. (*b*) Polystyrene at 180°C. The solid curves are calculations of the shear (lower curve) and biaxial elongational start-up curves using the generalized linear viscoelastic constitutive equation (see Chapter 8). The data shown were calculated using the positive biaxial strain rate $\dot{\epsilon}_B = -\frac{1}{2}\dot{\epsilon}$, and thus η_b in the figure is equal to $2\bar{\eta}_B$ (see Problem 5.18). *Source:* From the *Journal of Rheology,* Copyright © 1985, The Society of Rheology. Reprinted by permission.

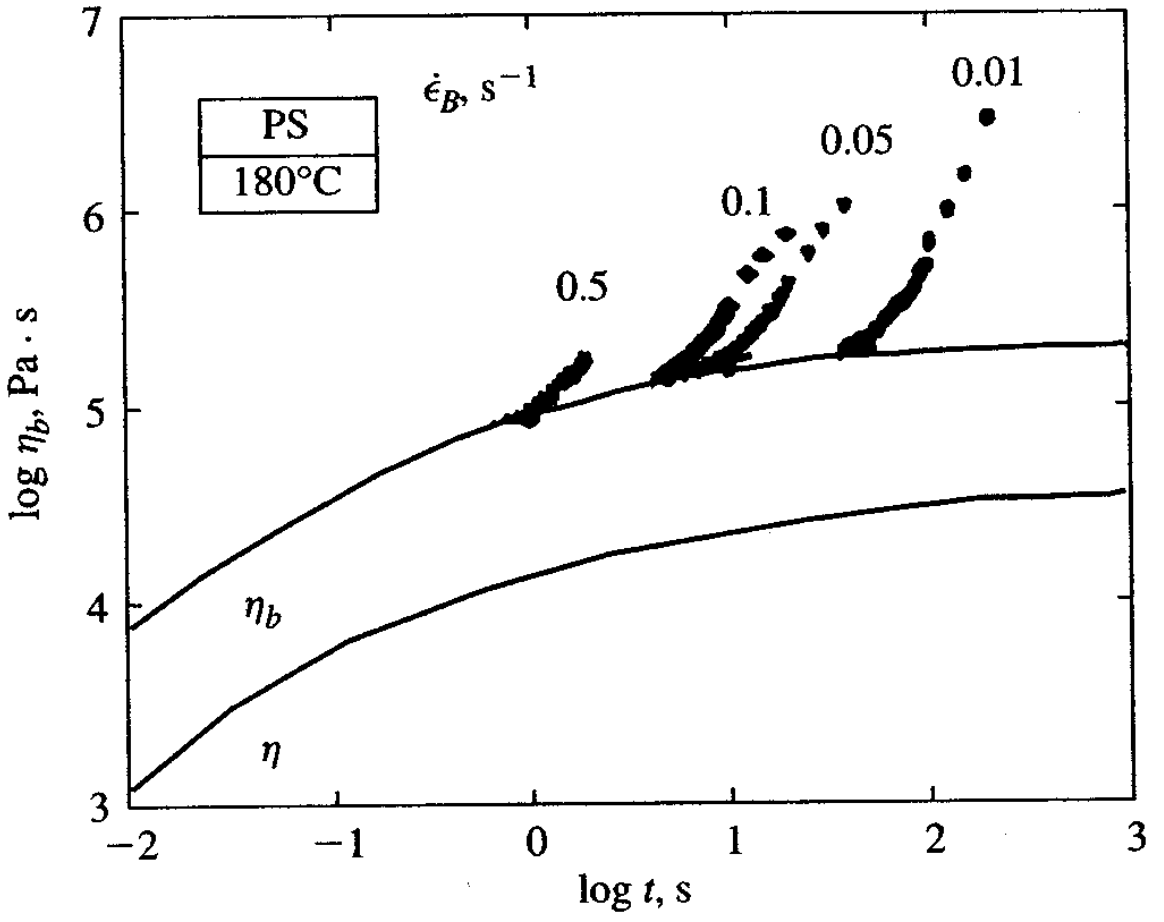

(*b*)

Figure 6.67 Continued

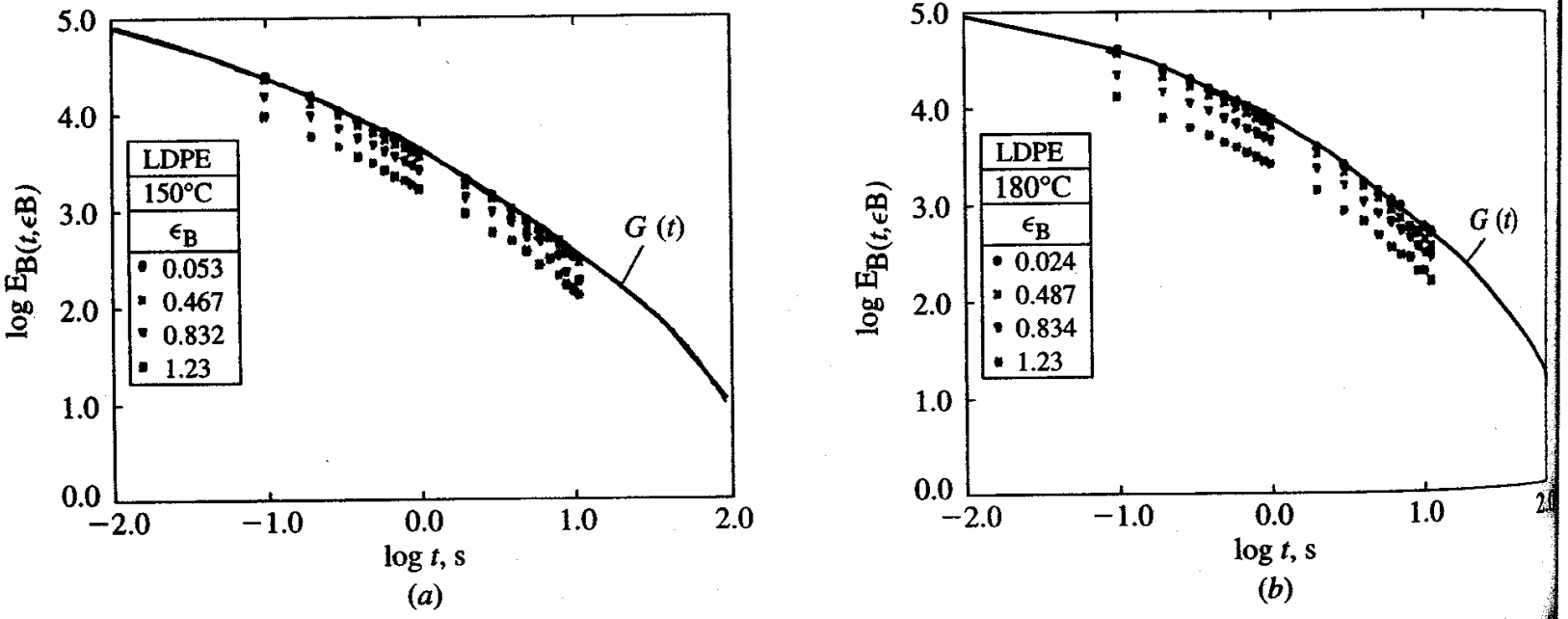

Figure 6.68 Nonlinear elongational stress-relaxation modulus $E_B(t,\epsilon_B)$, where $\epsilon_B = -\epsilon_0/2$, for (*a*) low-density polyethylene at 150°C and (*b*) polystyrene at 180°C; from Soskey and Winter [230]. At low strains the step-strain curves are independent of strain which is also observed in shear. *Source:* From the *Journal of Rheology,* Copyright © 1985, The Society of Rheology. Reprinted by permission.

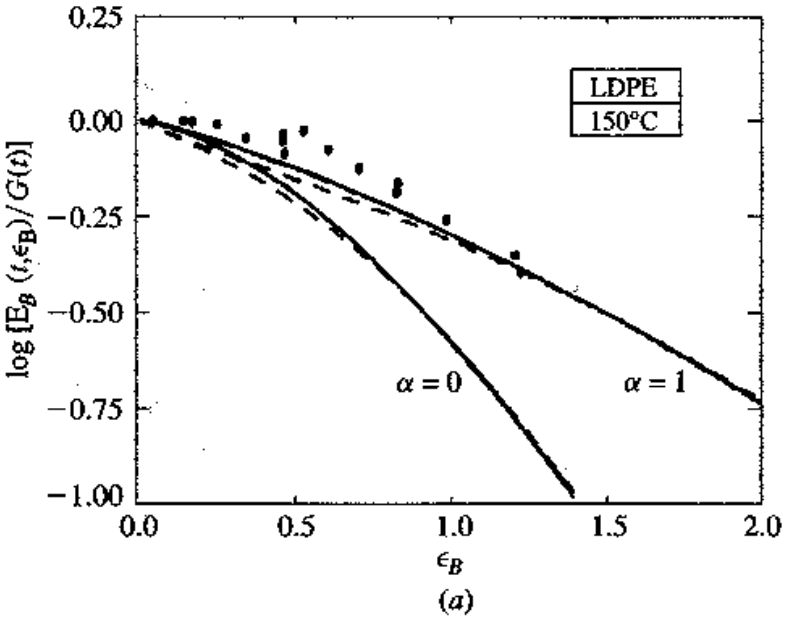

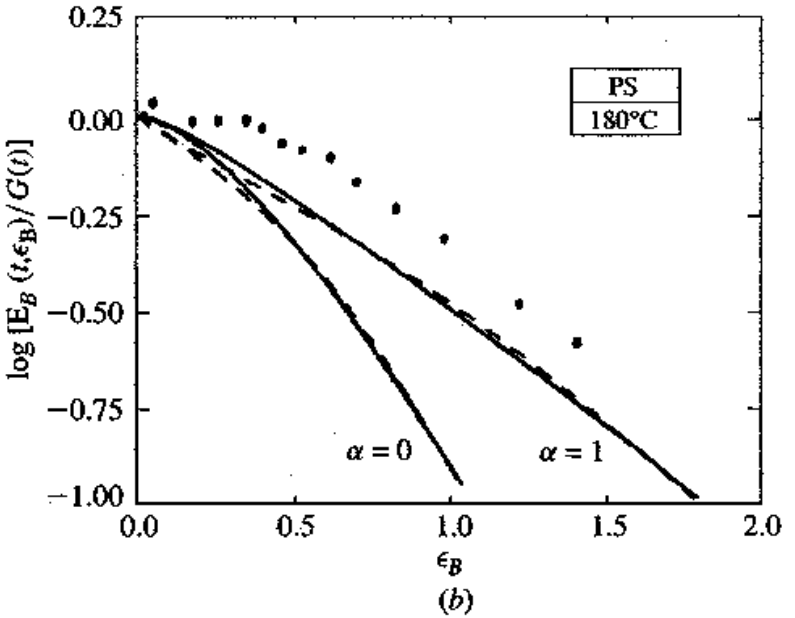

Figure 6.69 Step biaxial damping functions for (*a*) low-density polyethylene and (*b*) polystyrene calculated from the data in Figure 6.68; from Soskey and Winter [230] . The solid and dashed lines are empirical fits of the curves to the models of Soskey and Winter, where α is a parameter in their model, and $\epsilon_B = -\epsilon_0/2$. *Source:* From the *Journal of Rheology*, Copyright © 1985, The Society of Rheology. Reprinted by permission.